

W 34  
43484  
p. 35



# Performance of the 0.3-Meter Transonic Cryogenic Tunnel With Air, Nitrogen, and Sulfur Hexafluoride Media Under Closed Loop Automatic Control

S. Balakrishna and W. Allen Kilgore  
*ViGYAN, Inc., Hampton, Virginia*

N95-23257

Unclass

G3/34 0043484

Contract NAS1-19672

January 1995

National Aeronautics and  
Space Administration  
Langley Research Center  
Hampton, Virginia 23681-0001

(NASA-CR-195052) PERFORMANCE OF  
THE 0.3-METER TRANSONIC CRYOGENIC  
TUNNEL WITH AIR, NITROGEN, AND  
SULFUR HEXAFLUORIDE MEDIA UNDER  
CLOSED LOOP AUTOMATIC CONTROL  
(Vigyan Research Associates) 35 p



$x_{\text{chrg}}$	Heavy gas charging valve stroke, %
$x_{\text{recvr}}$	Heavy gas recovery valve stroke, %
$x_{\text{wv}}$	Water valve stroke, %
$x_{\text{rheo}}$	Speed control rheostat command, %
$x_{\text{exhaust}}$	Hydraulic tunnel exhaust valve stroke, %
$\alpha$	Angle of attack of the model
$\beta$	Fan inlet angles
$\gamma$	Ratio of specific heats of gas $\gamma=1.4$ for air/nitrogen $\gamma=1.1$ for SF6
$\lambda_i$	Local skin friction coefficient for ith segment
$\Delta T$	Temperature rise in heat exchanger, K
$\Delta P$	Pressure loss, atm
$\rho_i$	Density of gas in section i, $\text{kg/m}^3$
$\pi$	constant 3.14159
$\mu$	Viscosity of tunnel gas
mole	Molecular weight

## Abstract:

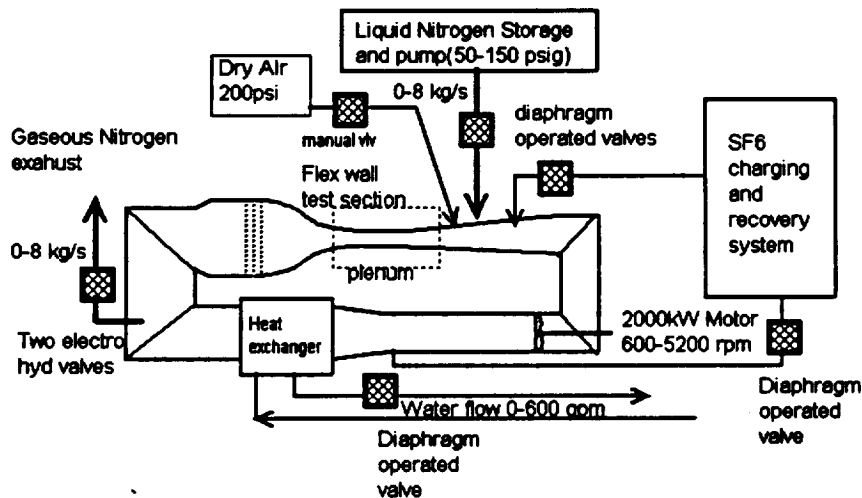
The NASA Langley 0.3-m Transonic Cryogenic Tunnel has been modified in 1994, to operate with any one of the three test gas media viz., Air, Cryogenic Nitrogen gas or Sulfur Hexafluoride gas. This document provides the initial test results in respect of the tunnel performance and tunnel control, as a part of the commissioning activities on the microcomputer based controller. The tunnel can provide precise and stable control in temperature to  $\leq \pm 0.3\text{K}$  in the range 80-320K in cryo mode or 300-320 K in air/SF6 mode, pressure to  $\pm 0.01$  psia in the range 15-88 psia and Mach number to  $\pm 0.0015$  in the range 0.150 to transonic Mach numbers up to 1.000. A new heat exchanger has been included in the tunnel circuit and is performing adequately. The tunnel airfoil testing benefits considerably by precise control of tunnel states and helps in generating high quality aerodynamic test data from the 0.3-m TCT.

## Nomenclature

A	Cross sectional area, $\text{m}^2$
$A_t$	Cross sectional area of test section, $\text{m}^2$
$A_r$	Aspect ratio of the model wing
$C_{L\alpha}$	Slope of lift curve for the model in the tunnel
$C_v$	Specific heat of tunnel gas at constant volume, $\text{kJ/kgK}$
$C_p$	Specific heat of tunnel gas at constant pressure, $\text{kJ/kgK}$
$C_w$	Specific heat of water, $\text{kJ/kgK}$
$D_i$	Diameter of $i$ th tunnel segment, m
$i$	Segment number of the tunnel
$k_{pp}$	Pressure loop proportional gain
$k_{pi}$	Pressure loop integral gain
$k_{tp}$	Temperature loop proportional gain
$k_{ti}$	Temperature loop integral gain
$k_{mp}$	Mach loop proportional gain
$k_{mi}$	Mach loop integral gain
$k_i$	Tunnel circuit loss factor for $i$ th segment
$k_\alpha$	Circuit loss due to model angle of attack
$L_i$	Length of $i$ th tunnel segment, m
$\dot{m}_w$	Water mass flow in the heat exchange, $\text{kg/s}$
$\dot{m}$	Mass flow, $\text{kg/s}$
M	Tunnel test section Mach number
$M_{\text{set}}$	Mach number set point
N	Fan speed, rpm
$N_{\text{set}}$	Fan speed set point, rpm
$N_{\text{com}}$	Fan speed command, rpm
P	Tunnel total pressure, atm(or psia)
$P_{\text{set}}$	Tunnel pressure set point, atm(or psia)
$\bar{q}_i$	Local dynamic pressure for $i$ th segment
$R$	Universal gas constant
$R_i$	Local flow Reynolds number/diameter
T	Tunnel total temperature, K
$T_{\text{win}}$	Water inlet temperature at heat exchanger, K
$T_{\text{out}}$	Water outlet temperature at heat exchanger, K
$T_{\text{set}}$	Tunnel gas temperature set point, K
$U, u_i$	One dimensional flow velocity, $\text{m/s}$

## Description of the 0.3-m TCT (Circa 1994):

The NASA Langley 0.3-meter Transonic Cryogenic Tunnel was established in 1973 and has evolved over the period of 21 years. The present test section is a 13 inch by 13 inch test section with top and bottom flexible walls and a plenum chamber enclosing the test section. The flexible walls are used to streamline the wall to minimize the aerodynamic wall interference effects by contouring them through 33 pairs of actuators so as to provide minimum wall interference. The tunnel is a closed circuit tunnel with a fan drive and the return leg sits below the testing leg, the whole tunnel being in a vertical plane. The fan outlet leads to a return leg diffuser terminating in to a heat exchanger. This heat exchanger was introduced in to the circuit in 1993-94 to allow heat removal during Air mode of operation and SF6 mode operation. The heat exchanger is made of cryogenic compatible material and hence can remain in the tunnel circuit during cryogenic nitrogen operation. During Cryo mode of operation, the heat exchanger is drained of water and connected to tunnel circuit to have minimal pressure difference. The tunnel flow from the heat exchanger is taken to the first corner and second corner. This is the section of tunnel with the largest diameter cross section. Control valves located in this section exhaust tunnel gas to atmosphere in Cryo mode or Air mode of operation. The second corner leads the flow in to a settling chamber. The screens in the settling chamber streamline the flow. The settling chamber leads into a contraction to accelerate the flow isentropically. The contraction terminates at the entrance to the test section/plenum chamber. The test section exit flow is taken through a high speed diffuser. Liquid nitrogen, air or sulfur hexafluoride is injected into the tunnel through appropriate control valves in this section. The diffuser exit flow leads to the third corner which in turn leads to the fourth corner. The fan shaft penetrates the tunnel at the fourth corner. The multibladed fan has a set of fixed inlet/outlet guide vanes.



0.3 Meter TCT and auxiliary systems  
for operation with three gas modes

As illustrated in the schematic above, there are (circa 1994) eight auxiliary service system essential in the operation of the 0.3-m TCT to operate with cryogenic nitrogen gas, air or sulfur hexafluoride. They are

## Introduction:

The NASA Langley 0.3-Meter Transonic Cryogenic Tunnel was established in 1973 (reference-1) to prove the concept that cooling the test gas in a closed circuit tunnel down to cryogenic temperatures results in enhanced Reynolds number and reduction in fan power for a given Mach number. With the emphasis on development of highly optimized transonic transport aircraft, during the waning years of 20th century, need for transonic aerodynamic wind tunnel testing which also accounted for proper Reynolds number similitude was considered a high priority. In cryogenic tunnels, the flow Reynolds number can approach real flight values for subscale models at desired Mach number. Nitrogen, a major constituent of air is used as the test media and the tunnel is cooled by injection of liquid nitrogen which evaporates into the test gas. Warmer excess gas is removed from the tunnel to atmosphere. This concept also allowed independent control of tunnel dynamic pressure, and Reynolds number at any desired Mach number. The proof of concept demonstrated at the 0.3-m TCT lead the way to establishment of the National Transonic Facility in United States (reference-2) and the European Transonic Wind Tunnel at Cologne, Germany. Testing for aerodynamic design in the cryogenic tunnels have shown instrumentation problems associated with thermal stability.

The concept of using high molecular weight gas to enhance the flow Reynolds number at ambient temperatures is an alternative to the cryogenic tunnel concept. At NASA Langley Research Center, a program to modify the 0.3-m TCT to function with three different test gases, namely cryogenic nitrogen, dry air and sulfur hexafluoride was initiated in 1991. This program allows comparison of experimental high Reynolds number aerodynamic data using cryogenic nitrogen as well as sulfur hexafluoride. Questions about the viability of SF<sub>6</sub> as a wind tunnel test gas including its real gas effects remain and these need to be experimentally answered by comparing results from two different gases on same model. A project was initiated at NASA Langley to modify the 0.3-m TCT to function with either cryogenic nitrogen/air or heavy gas sulfur hexafluoride. During 1992-1993 period, amongst many other design and development activities, a modeling and control study of the 0.3-m TCT for use with sulfur hexafluoride medium was made. The aim was to quantify the performance and hence the associated control system changes (reference-3). This study also included the possibility of operating the tunnel with air as the test medium. Both these gases, SF<sub>6</sub> and air, required configuration changes involving addition of a heat exchanger in the return leg of the tunnel circuit to allow removal of fan induced heat (such a feature was not required for cryogenic operation). A control system was designed so that the tunnel could work with any one of the three gases. Introduction of the heat exchanger affects the cryogenic mode tunnel circuit loss characteristics. Reference-3 presents the mathematical modeling of the tunnel, dynamical simulation, development of closed loop control law and control hardware change required for operation with sulfur hexafluoride test gas, air and cryogenic nitrogen gas. It also presents design changes to the cryogenic mode tunnel controller working since 1988 (references 4 and 5) to accommodate the change of gases and still provide robust tunnel control in the presence of strong thermodynamic interaction typical of closed circuit tunnels.

During 1994, the 0.3-m TCT was recommissioned to function with all the three gases. This document presents evaluation of the tunnel performance and control system during the closed loop control operation of 0.3-m-TCT in all the three gas modes. It presents the automatic control code used in the microprocessor based controller as appendices II, III and IV. It also compares the tunnel performance with all the gases.

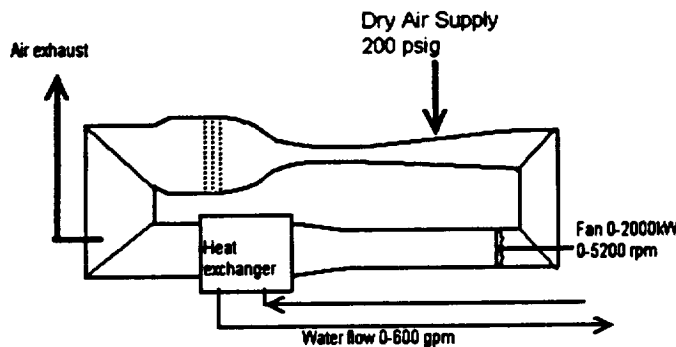
The tunnel gas discharge system consists of two electrohydraulically operated globe valves to control flow from the big end of the tunnel and allows venting of the air or gaseous-cold nitrogen to the atmosphere through a vent stack. The valves are capable of full stroke motion in less than a second. They provide tunnel control effectively. These valves are used in Cryo mode as well as the Air mode of tunnel operation. This system is interlocked to be non functional during the SF6 mode so as to prevent discharge of SF6 to atmosphere.

A heat exchanger was introduced in the tunnel circuit during 1993-94 period to allow heat removal while in Air mode or SF6 mode of operation. This device is serviced from a cooling water supply system capable of 600 gpm flow at pressures upto 60 psig. A throttle type remotely operated diaphragm actuated water flow control valve has been used to control the water mass flow in to the heat exchanger so as to control the tunnel gas temperature.

A ninth ancillary system is the closed circuit boundary layer suction control system is available, but is not presently operational. This system has been demonstrated (reference-3) to be capable of removing upto 4-10% of the test section mass flow (depending on the test section Mach number) and reinject the same mass in to the tunnel at the down stream high speed diffuser.

### Commissioning tests on the 0.3-m TCT in post SF6 operational modifications

#### Air mode commissioning with heat exchanger in circuit:



#### 0.3-Meter TCT in Air mode

The figure above illustrates the tunnel and the support auxiliary systems used for air mode of operation. The initial tests conducted were the closed loop air pressure control tests. The source of air is building service air at 200 psig, which is released into the tunnel circuit continuously at a low rate of mass flow of about 0.1 lb/s. This is presently performed manually whenever Air mode operation is required. The tunnel builds up air pressure. The hydraulically operated discharge valves are used to remove excess air and control the tunnel pressure automatically. A newly developed control subroutine 'AIR', is used to perform this control task. The pressure control law consists of a proportional integral control law with gain scheduling.

$$x_{\text{exhaust}} = \frac{750}{P\sqrt{T}} \left\{ (k_{pp}(P-P_{\text{set}}) + k_{pi} \int (P-P_{\text{set}})) \right\}$$

1. Fan drive motor, common for all gas modes,
2. Liquid nitrogen pumping/storage system, used only for cryogenic nitrogen mode,
3. Two diaphragm operated pneumatic valves, used in cryo mode,
4. Sulfur hexafluoride supply and recovery system used for heavy gas mode,
5. Dry Air supply used in Air mode,
6. Two electrohydraulic tunnel gas discharge valves, used in cryo and air modes,
7. Heat exchanger water supply and return valves, used in SF6 and air modes,
8. SF6 supply valve and SF6 recovery valves, used in SF6 mode.

The 0.3-m TCT consists of the drive motor which is a squirrel cage water cooled two pole induction motor driven by a variable frequency generator (10-120 Hz) having a voltage frequency ratio of 35 v/Hz. The tunnel fan shaft penetration has a seal and oil cooled bearings which can be kept hot while in cryogenic operation. The 0-5600 rpm variable speed motor drives a fixed 12 bladed fan impeller with fixed guide vanes and yields the necessary pressure ratio to sustain the tunnel flow. The fan drives all the three gases, nitrogen, air or SF6. The maximum speed in SF6 mode necessary is only about 2300 rpm where as in Air mode, the fan speed required is upto 5200 rpm for transonic Mach number. The Cryo mode fan speed requirement varies from 5200 maximum at 310 K down to about 2500 at 80 K.

A liquid nitrogen storage system with two large vacuum jacketed storage tanks feed a liquid nitrogen pump. The pump flow of 5-10 kg/s at pressures variable from 50 to 160 psig, is taken around the tunnel circuit and the unused liquid nitrogen flow is returned to the tank through a remotely controlled diaphragm operated pneumatic pressure relief valve. This valve can control the liquid nitrogen supply pressure to the tunnel.

A second set of remotely operated diaphragm type valves, under control of tunnel automatic control, can inject desired amounts of liquid nitrogen into the tunnel, from the liquid nitrogen supply bus. The liquid nitrogen valves are interlocked so that liquid nitrogen valves do not operate while on SF6 mode.

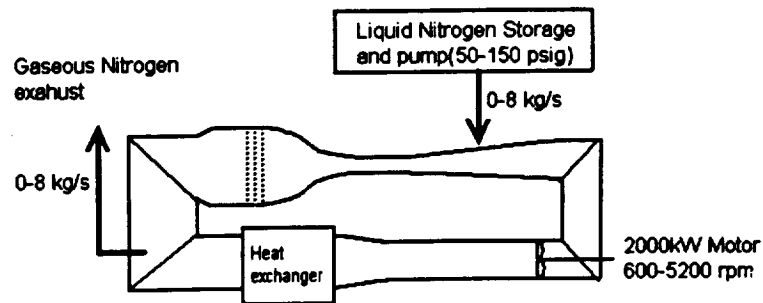
Sulfur hexafluoride is stored in the liquid form in a supply/recovery system. This self contained supply and recovery unit can supply sulfur hexafluoride to the tunnel by boiling and evaporating stored SF6. Return gas can be compressed and refrigerated to liquefy the gas for storage. The supply/recovery system is a complex modular system. The closed circuit SF6 system has been designed to minimize the leakage of SF6 gas to atmosphere, as the heavy gas has the potential to be an environmental hazard as a green house effect gas. Environmental Protection Agency guide lines dictate the maximum leak rate allowed.

Two pneumatically controlled remotely operated diaphragm valves are used to charge the tunnel or to recover, liquefy and store SF6. The charge and discharge rates of the SF6 into and out of the tunnel is very slow, charge being about 0.275 kg/s and the discharge rate is about 0.138 kg/s because of the compressor/refrigeration capacity.

Provision also has been made to connect dry process air in to the tunnel. This is performed through a manually controlled valve and continues to charge the tunnel with a steady air mass flow as long as the tunnel is functioning in Air mode. Excess air is removed by the tunnel controller as a part of the pressure control law through the electrohydraulic discharge valves.

steady state conditions to within  $\pm 0.3$  K around the set point till its capacity is exceeded. This occurs when pressure reaches 45 psia and the Mach number exceeds 0.680. Under these conditions, the water valve is full open at 100%. The trajectories also demonstrate the controller performance with cross coupling between the three loops.

Cryogenic mode recommissioning with heat exchanger in circuit.



**0-3 Meter TCT in Cryogenic Mode**

The figure above illustrates the auxiliary systems used in Cryo mode of the tunnel operation. In this mode, the tunnel was run directly using the control code 'CRYO', using same procedures used before the tunnel modifications for heavy gas/air were made. The control code is essentially same as the one used prior tunnel to modifications. The control laws are robust enough to accommodate extra circuit losses due to the inclusion of the heat exchanger in the circuit. Precaution taken were to dry out the heat exchanger and connect it to the tunnel stream to reduce the pressure difference between stream and the heat exchanger. All the SF6 gas system piping was secured shut from the tunnel as was the air supply line. The tunnel fan speed-Mach relation, tunnel gas and structural cooling rates and other system characteristics remained largely the same as before. The effect of extra circuit losses due to the heat exchanger was not very evident in the tunnel operation either as increased fan speed or motor current. Since the test section flexible walls are used, the Mach number/fan speed relation varies as a function of model blockage and the flexwall contouring program. Hence the variations in fan speed-Mach relation is not repeatable. Minor changes in the fan speed/Mach relation which were observe could not establish whether these changes were due to inclusion of the heat exchanger or the flex wall reconfiguration. Post modification Cryo mode tunnel response plots are shown in the figure 2. The test illustrated shows a series of temperature steps conducted while evaluating infrared sensor based flow visualization equipment.

The figure 2 shows a cryogenic run performed with modified code and the heat exchanger in the circuit on March 8, 1994. The tunnel run with cryogenic nitrogen starts at ambient temperature of 300K, tunnel pressure of 17 psia and Mach number of 0.260. The tunnel pressure has been raised to 20 psia while increasing Mach number to 0.600 through steps 0.400, 0.450, 0.500 and 0.550. The tunnel temperature has been taken from 250K to 200 K in about 25 steps, and 200K to 100K in about 50 steps. The stability of pressure and Mach number can be seen from the trajectories. The control accuracy is  $\pm 0.3$ K in temperature,  $\pm 0.01$  psia in pressure and  $\pm 0.0015$  in Mach number.

In the initial tests, the pressure control was realized without the fan being operated. The tunnel pressure loop control law was fine tuned to hold the desired pressure in the range of 16 to 80 psia to an accuracy of  $\pm 0.01$  psia around the set point.

The Mach control loop required no modifications as the gaseous nitrogen and air are very similar in character and hence the fan speed/Mach relationship remains the same. Hence there was no need for any fine tuning of the Mach loop, which was a copy of the original loop control law operated at 310K.

$$x_{rheo} = \frac{520\sqrt{T}(1-0.5M)}{p^{0.035}} \int (N_{com}-N) \quad \text{with minimax clip} \quad -\frac{\sqrt{T}}{20} < (N_{set}-N) < \frac{\sqrt{T}}{20}$$

$$\text{In Mach loop, } N_{com} = k_{mp}(M_{set}-M) + k_{mi} \int (M_{set}-M)$$

$$\text{In Speed loop } N_{com} = N_{set}$$

The second step then was to commission the heat exchanger circuit together with the Mach number control loop. This part of control code is new and utilizes a feedforward of fan power in terms of equivalent water mass flow, based on 36-40 kg/s for 100% opening of the water flow control valve. The closed loop temperature control law is

$$x_{wv} = \frac{5 P \left( \frac{N}{1000} \right)^{2.26}}{\sqrt{T} (T_{set} - T_{win})} + k_{tp}(T - T_{set}) + k_{ti} \int (T - T_{set})$$

The controller senses the tunnel stream temperature (T) through the chromel alumel T25 thermocouple. The controller manipulates the cooling water mass flow. If the desired temperature set point ( $T_{set}$ ) is higher than tunnel gas stream temperature, more water is allowed in and viceversa. The temperature sensor is the tunnel stagnation temperature sensor common to all modes of operation.

The fan speed drive was brought on and was initially tested at constant fan speed while holding tunnel pressure constant. The temperature loop gains were tuned to provide good temperature control. This was tested by changing the tunnel Mach number at constant pressure. The feedforward from the fan power estimates was also tuned. The temperature loop was evaluated upto nearly 450kW of power, by operating the tunnel in the Air mode at 45 psia,  $M=0.700$  and a temperature of 312K. Some initial commissioning responses of the Air mode operation are illustrated in figure 1.

Figure 1 show the pressure control, temperature control and Mach number capability of the controller in Air mode conducted on February 24, 1994. The tunnel pressure set points are 20, 32, 35 and 40 psia. The rate of pressure rise is dictated by amount of air entering the tunnel which is manually set by the operator. Under stable pressure conditions, this air mass flow is exhausted out through the hydraulically operated vent valve. The starting Mach number is 0.100 and has been increased in steps through 0.500, 0.680, 0.500, 0.600, 0.700, 0.730 and 0.750. The tunnel temperature set points were 293 K, 302 K and 312 K. The pressure stability is better than  $\pm 0.01$  psia around the set point, where as the Mach number accuracy is  $\pm 0.0015$  around the set point. The temperature loop is the slowest, but still maintains temperature under

The first step in the commissioning was to operate the SF6 vaporizer/injection route simultaneously with the recovery compressor/refrigeration system. This test was performed without having to run the fan or the cooling water system. The tunnel pressure control law was fine tuned and checked upto 50 psia to an accuracy of better than  $\pm 0.01$  psia of the set point. The second step involved simultaneous operation of the fan drive and the cooling system. Since the fan sensitivity is totally different for SF6 mode, the fan speed control was checked first and then the Mach loop. This mode of operation requires a maximum speed of about 2400 rpm for  $M \approx 1$ . The Mach loop was fine tuned to provide Mach stability of  $\pm 0.0015$  around the set point.

The temperature loop was fine tuned later to realize a set point control and temperature accuracy of  $\pm 0.1K$  (Much better than the aimed  $\pm 0.5K$ ). The feedforward portion of the temperature loop was also fine tuned. Typical tunnel response characteristics are shown in figures 3 through 7.

Reference 3 details the predicted estimation of the modified 0.3-m TCT with sulfur hexafluoride test medium and thermodynamic modeling was detailed. The mathematical modeling and its dynamical simulation led to generation of predicted tunnel performance as follows have been presented in reference-3.

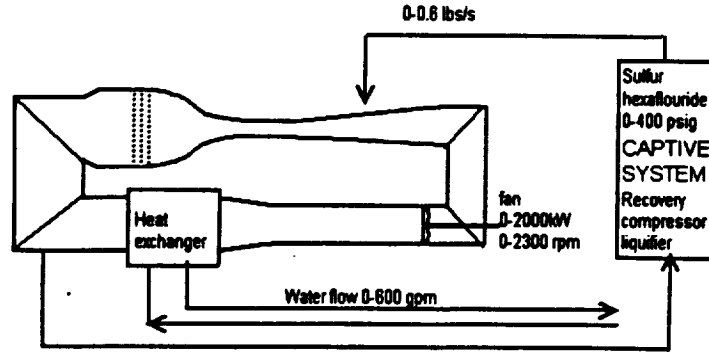
1. Fan speed-Mach number relation based on fan performance.
2. Fan power-Mach number relation based on tunnel water temperature rise.
3. Heat exchanger model and tunnel temperature dynamics.
4. Tunnel pressure dynamics.
5. Tunnel control law synthesis and simulation.

In this section, the estimated performance from reference-3 and the experimental commissioning results are compared. The tunnel experimental performance was obtained from a recording of the tunnel time trajectories during initial commissioning runs.

#### *0.3m TCT fan speed-Mach relationship in SF6 mode*

Figure 3 shows the fan speed Mach number relationship from first four SF6 mode runs. The experiments were conducted with an airfoil model and flexwalls continuously adapting for different optimum Mach numbers, where as the predicted fan speed plot from reference 3 is based on empty test section. The experimental plots show dark spots at which condition the tunnel was run for long periods ( $M=0.700$  and  $0.500$ ). The predicted curve is parallel to experimental plots but is slightly above. The shift is about 130 rpm. The experimental plots which vary amongst themselves. The likely reason for the shift is that the effective test section area is less than  $0.109 \text{ m}^2$  used in the simulation and prediction. The flexwall activity for different Mach numbers and angles of attack have created a band of fan speed. The tunnel choked beyond Mach 0.710 due to the airfoil characteristics. The tunnel pressure was varied from 20 to 50 psia with very little effect on the fan speed-Mach number relation. In summary, the predicted fan behavior (from reference-3) agrees quite well with the experimental fan speed results, validating the modeling and the mass flow identities of reference 3.

## Heavy gas SF6 Mode commissioning



The figure above illustrates the schematic of the SF6 mode. While commissioning the SF6 mode, the first need was to evacuate the tunnel to 0.3 psia. Lower vacuum level could not be easily realized. This accounts for about 0.33 kg of air in the tunnel circuit, compared to about 85 kg of SF6 at one atmosphere charge, amounting to a concentration of 99.5% by weight at 1 atm.

The control code used in the heavy gas sulfur hexafluoride mode has been developed and tested. This control code uses control laws which are different from the other two modes. The pressure control law for charging and recovery are

$$x_{\text{chrg}} = \frac{1500}{P\sqrt{T}} \{ k_{\text{pp}}(P_{\text{set}} - P) + k_{\text{pi}} \int (P_{\text{set}} - P) \}$$

$$x_{\text{recvr}} = \frac{1000}{P\sqrt{T}} \{ k_{\text{pp}}(P_{\text{set}} - P) + k_{\text{pi}} \int (P_{\text{set}} - P) \}$$

The temperature control law, based on use of water mass flow control is

$$x_{\text{wv}} = \frac{15.9 P M^3}{20(1 + \frac{\gamma-1}{2} M^2)^{\frac{\gamma+1}{2(\gamma-1)}} (T_{\text{set}} - T_{\text{win}})\sqrt{T}} + k_{\text{tp}}(T - T_{\text{set}}) + k_{\text{ti}} \int (T - T_{\text{set}})$$

The Mach number control law is different from the air/cryo modes and is

$$x_{\text{rheo}} = 251\sqrt{T}(1-0.8M) \int (N_{\text{com}} - N) \quad \text{with minimax clip} \quad -\frac{\sqrt{T}}{20} < (N_{\text{set}} - N) < \frac{\sqrt{T}}{20}$$

$$\text{In Mach loop, } N_{\text{com}} = k_{\text{mp}}(M_{\text{set}} - M) + k_{\text{mi}} \int (M_{\text{set}} - M)$$

$$\text{In Speed loop } N_{\text{com}} = N_{\text{set}}$$

second case the tunnel is at equilibrium at 29.8 psia, temperature at 309K and Mach number at  $M=0.500$ . The tunnel pressure set point is commanded to 20 psia. The tunnel temperature shows a mild dip transiently, but is quickly brought back to 309K. The tunnel Mach number remains steady at 0.500 and the recovery system slowly reduces the tunnel pressure in about 800 s (0.6 psi/minute).

### Heat Exchanger performance and tunnel power consumption in air and SF6 modes:

The heat exchanger introduced in to the tunnel circuit was designed based on certain estimates of tunnel pressure losses and heat exchange capabilities. Specifically, the heat exchanger was designed at a maximum mass flow of 320 kg/s, dynamic pressure of 0.152 psi, and total pressure of 6 atm (88 psia),  $M=0.9$  to have a local  $\Delta P/\bar{q}_{local}=4.6$  or  $\Delta P=0.7$  psi, as detailed in reference 7. The heat exchanger has been designed for mean temperature difference of 30K between mean water and gas temperature, to remove 750kW at a tunnel mass flow of 260 kg/s of sulfur hexafluoride gas with the tunnel total pressure at about 5 atm(74 psia).

In terms of the heat exchange, at a temperature rise of water by 4K at full mass flow of about 600-660 gpm or 36-40 kg/s, the heat removed is about 650 kW. From the various cases of air mode and SF6s mode operations, considerable amount of data was gathered in respect of tunnel conditions and on the temperature rise. The power removed by water is determined as

$$\begin{aligned} \text{power} &= \dot{m}_w C_w \Delta T \\ \text{where } \dot{m}_w &= 36-40 \text{ kg/s at 100\% valve} \\ C_w &= 4.2 \text{ kJ/kg/K} \end{aligned}$$

All the power estimates are based on water temperature rise under near steady state conditions. A comparison of the power estimate from the tunnel simulation is made with power estimates based on heat removed by water in the heat exchanger. Figures 8, 9, 10 and 11 show the comparison. Two cases correspond to air mode operation when the tunnel was run at different Mach numbers at 45 and 75 psia. In Figure 8, results of air mode operation at 45 psia are compared with simulation. The simulation and experimental fan speed match is very good. The fan power simulation and experimental numbers also match reasonably well. It should be noted that the heat removed by water does not correct for residual heat absorption by the 3000 kg of aluminum which has a time constant of nearly 600 seconds. Further, the tunnel geometry has been continuously changed in the various experimental data by flex wall operation at different angles of attack. Figure 9 shows similar match in speed and fan power for 75 psia tunnel pressure case. The figure 10 shows the SF6 mode data when the pressure is 4.3 atm(63 psia).

Figure 11 compares the air mode power versus SF6 mode power. Since the experiments were performed at different pressures, the figure shows the power normalized to tunnel pressure in Y-axis and Mach number in X-axis. The estimated power from simulation is also shown. For a given pressure and Mach number, the power consumed by tunnel in SF6 mode is typically about 40% of the air mode, as can be expected from theory. The experimental results are lower than theoretical estimates, and as was discussed before, heat absorption by walls and possible overestimate of tunnel circuit loss factor can explain the difference.

### *Tunnel temperature dynamics and water flow valve*

The convection heat transfer efficiency of the heat exchanger introduced into the 0.3-m TCT circuit has been checked by comparing the static performance as well as the transient response. Figure 4 shows a set point change during tunnel equilibrium conditions. The tunnel was brought to equilibrium conditions at 307K, 29.75 psia and  $M=0.712$ . Then the temperature set point was changed to 309 K. The water valve uses a feedforward and drops from 80% valve opening to 40% and slowly adjusts the mass flow to regulate temperature. The temperature step takes about 30-40 seconds to reach the temperature control band of 0.3K. It may be noted that the tunnel pressure increases from 29.75 upto about 29.85 due to increase of temperature. The recovery valve pulls in the extra mass slowly and takes nearly 250 seconds to reach equilibrium. However, the pressure reaches the error band in less than 40 seconds and is ready for data acquisition. The tunnel Mach number is not affected by the temperature change, while the fan speed moves very slightly from 2030 to 2035 to accommodate the temperature increase. The Mach number remains to within 0.0015 of set value through out the temperature step period. The temperature control accuracy is  $\pm 0.1K$  around the set point at steady state conditions, and is better than the design goal of  $\pm 0.5 K$ .

### *Tunnel Mach number dynamics and fan speed control*

The tunnel fan speed control Mach number. The results of tunnel control from July 15, 1994 is illustrated in the figure 5. The tunnel was first brought to equilibrium conditions at 30.1 psia,  $M=0.705$  and temperature of 309.0K. The fan speed required for equilibrium is 2130 rpm, water valve at about 58%. The tunnel Mach number set point is changed to 0.500. The Mach number settle out to 0.500 in about 30 seconds. The reduced fan power drops temperature transiently to 308.2K, and the water valve drops back to about 20%. By the time the Mach number settles, the temperature is also back to 309K. The tunnel pressure also drops to 29.8 psia during the temperature transient and Mach transient. The charge valve injects new mass to the circuit and builds the pressure back to about 30.5 psia. The plot also shows a Mach correction to  $M=0.505$  from 0.500 and a pressure correction from 30.1 to 29.85 psia, with the recovery valve active. The recovery cycle is active for nearly three minutes though the tunnel is at the set point within 30-40 seconds after all operator commands have ceased. In summary the the coupled close loop system responds to Mach set point change and effectively corrects the coupled pressure/temperature transients. The Mach number stability is within  $\pm 0.0015$  of the set value over long periods.

### *Pressure dynamics and charge/recovery valve control*

The closed loop pressure control law uses the charge valve to increase tunnel resident gas mass for increase of pressure, during which time the recovery valve is kept closed. The control law uses the recovery valve, which takes the flow into the suction of a compressor whose output is cooled and gas is refrigerated. The charge valve is kept closed while the recovery valve is functional. Examples of tunnel pressure increase and decrease are shown in figures 6 and 7. The pressure control accuracy is within  $\pm 0.08$  psia while the root mean squared disturbances are a little higher at  $\pm 0.1$  psia due to noise in the line. In the first case, the tunnel pressure was progressively builtup from 16 psia, 20 psia, 30 psia, 40 psia and 50 psia while the Mach number was increased in steps 0.500, 0.600 and 0.700/0.710. The temperature loops was closed only after 600 seconds and it maintains temperature while the pressure is ramped through 20/30/40 and 50 psia. This situation corresponds to first commissioning runs for the SF6 mode. In the

**Table I : Controller Sensor/Actuator signals**

Input name	Sensor	Range	Volt/amps
E(1)	PP (P)	0-100 psia	0-5 VDC
E(2)	PS (P <sub>s</sub> )	0-100 psia	0-5 VDC
E(3)	TT (T)	78-342 K	0-5 VDC
E(4)	TMWL(T <sub>m</sub> )	78-342 K	0-5 VDC
E(5)	FRPM (N)	0-6400 rpm	0-5 VDC
E(6)	PLQ	0-300 psig	1-5 VDC
E(7)	DLP	0-5 psid	0-5 VDC
E(8)	-	-	-
E(9)	PSF (P <sub>sf</sub> )	0-200 psia	0-5 VDC
E(10)	RSF (P <sub>b</sub> )	0-100 psia	0-5 VDC
E(11)	TWI (T <sub>w</sub> )	273-330 K	0-5 VDC
E(12)	TWO (T <sub>h</sub> )	273-330 K	0-5 VDC
E(13)	SFCN (κ)	50-100%	0-5 VDC
E(14)	PST(P <sub>st</sub> )	0-1000 psig	0-5 VDC
E(15)	-	-	-
E(16)	-	-	-
Output name	Actuator	Range	drive
DAC(1)	ALQ	0-100%	4-20 ma
DAC(2)	ALQ	0-100%	4-20 ma
DAC(3)	ALN	0-100%	0-5 VDC
DAC(4)	AGV1	0-100%	1-5 VDC
DAC(5)	AGV2	0-100%	1-5 VDC
DAC(6)	SNRPM	0-6400	0-5 VDC
DAC(7)	IQ	Fan ref	5 VDC
DAC(8)	-	-	-
DAC(9)	AISF	0-100%	4-20 ma
DAC(10)	AOSF	0-100%	4-20 ma
DAC(11)	AWV	0-100%	4-20 ma
DAC(12)	-	-	-

Sensors for cryogenic tunnel and all except PLQ will be required for SF<sub>6</sub> gas operation also

Sensors for SF<sub>6</sub> gas tunnel

Actuator drives for Air and cryo modes. Only SNRPM/ IQ will be used in SF<sub>6</sub> gas operation ( SNRPM = 500-2500 rpm for SF<sub>6</sub>)

Actuator drives for the SF<sub>6</sub> mode of operation

Figure 12 shows a typical simulation plot for the cryogenic mode of operation. No experimental results are presented in this figure 12, as there was no major change in the cryogenic performance of the tunnel after modifications.

### **0.3-Meter Transonic Cryogenic Tunnel Controller:**

The microprocessor based tunnel controller of circa 1987 was modified to function for all the three modes of tunnel gas. The math modeling and control law development details are presented in reference 3. The control code evolution was on the same as the lines used in 1987 code which has provided trouble free performance for nearly six years now. The control law codes have been compiled and executable codes are available for use. All the three control laws have been thoroughly tested and have yielded excellent control.

Modifications to accommodate new gases involved addition of a set of sensors to communicate tunnel states to the controller and actuators to be driven by the controller. The details of the new sensor/controller wiring used are shown in table I. The new wiring details are presented in figure 13. It shows signal inputs for 13 sensors, and drives all the seven actuators discussed previously. The details of the I/O devices are provided in reference 3.

The controller now has three control codes called 'Cryo', 'Air' and 'SF6'. On a power off booting of the controller, the screen provides the choice of these three control codes. The control codes are detailed in Appendices II, III and IV (Corresponding to Cryo mode, Air mode and SF6 mode).

### **Concluding Remarks:**

The 0.3-Meter Transonic Cryogenic Tunnel has been modified to work with three different gas media viz., cryogenic nitrogen gas in temperature range 80-310K, ambient temperature air and ambient temperature sulfur hexafluoride. This modification involved introduction of a heat exchanger to remain permanently in the tunnel circuit. Because of these changes, the tunnel closed loop controller to hold pressure, temperature and Mach number had to be modified and the tunnel recommissioned.

This document has presented the 0.3-meter Transonic Cryogenic Tunnel operation under closed loop control with the three different gas media. The tunnel control accuracy remains  $\pm 0.01$  psi in pressure,  $\pm 0.1$  to  $\pm 0.3$  K in temperature and  $\pm 0.0015$  in Mach number. The heat exchanger is performing as designed with both the circuit loss coefficient and heat exchange efficiency adequate. The three closed loop control codes are performing very well as illustrated by various figures. The tunnel circuit losses have increased and the estimated increase of losses agree with the experimental performance.

### **Acknowledgment**

This work has been performed under NASA contract number NAS1-19672, Task 25 with John B Anders as the task monitor. The authors acknowledge the technical support received in the successful completion of the controls work, from 0.3-m TCT team led by Stu Flechner.

solution to continuity equation, energy equation and momentum equation simplified for one dimensional flow. The simulation methodology was developed to treat any endless duct with a compressible gas whose thermophysical properties are known. A generalized fan has been used with a single stage rotor and inlet/outlet guide vanes which can be moved. This simulation is performed on a MATLAB platform.

The 0.3-m TCT is a fan driven pressure tunnel, with either water cooled heat exchanger or a cryogenic nitrogen spray. The test medium being considered is air/nitrogen with its well known calorically and thermally near perfect behavior and minimal real gas effects. The tunnel, will also use heavy molecular weight gases with their advantages of higher Reynolds number capability with lower ratio of specific heats resulting in much reduced power requirements. In the first analysis, only air is considered as the test medium. The flow of captive gas in a closed circuit can be represented by well known compressible gas duct flow equations of continuity, momentum, energy and state with isentropic relations. Since the area of the endless tunnel duct changes around the circuit, the duct flow solutions change spatially. Further, to account for transit time temporal effects and the spatial effects need to be analyzed in time dimension also.

The 0.3-m TCT has been considered as a 48 segment endless duct with a fan. Ideally, this number can be much larger. The breakup used in the present analysis is shown in Table I. The test section has been treated as a 5 element cascade. Each segment is associated with a volume, an area of cross section, a local circuit loss factor based on Reynolds number, transverse mass removal or mass addition (in the case of the test section with porous walls, the reentry stations, tunnel mass addition or removal terms), and energy addition or removal term. To establish the tunnel spatial pressure, temperature and Mach number profiles, the duct flow compressible equations of continuity, momentum, energy and related isentropic identities have been used. A fan module is essential for completing the compressible flow analysis. The basic driver for the analysis is an adjustable mass flow term and the starting captive gas mass in the circuit. The temperature establishes the initial pressure.

Given an initial mass flow, The total/static temperature distribution is found for segment 1 by solving the relevant equations of continuity, momentum and energy. The energy increment occurs due to wall heat release, in the heat exchanger segment and the fan segment. The local mass flow rate, static pressure and local loss factor provide the total pressure loss in the segment due to momentum effects. This solution now provides the inlet conditions to segment 2. A tunnel state profile can thus be had for the first 25 segment when the mass flow rate, initial pressure and temperature at the fan exit are given. The exit conditions of segment 25 constitute the inlet to the fan. Mach number is obtained by solving for  $M(i)$  in the following equation together with associated isentropic relations, momentum and energy relations relevant to particular module.

$$\dot{m}(i) = \rho_k \sqrt{\frac{\mathfrak{R}\gamma}{\text{mole } T(i)}} \frac{P(i)M(i) A(i)}{(1 + \frac{\gamma-1}{2}M^2(i))^{\frac{\gamma+1}{2(\gamma-1)}}$$

for air/nitrogen  $\gamma=1.4$  for SF6  $\gamma \approx 1.1$

With  $\gamma=1.4$ , the above equation is a sixth order equation with two real roots and four complex roots. The two real roots correspond to subsonic and supersonic solutions.

# Appendix I

## Tunnel Performance Simulation

The circuit loss pattern of the tunnel circuit remains constant for all the three gases used. The loss factor has been discussed in some detail in reference 3. Inclusion of the heat exchange with its extra circuit loss is the modified version compared to 1980's version of the tunnel. The loss factor is discussed in the foregoing section, and a tunnel flow mathematical simulation has been performed using a generic tunnel simulator. The 0.3-m TCT circuit has been defined as consisting of 48 cylindrical/cone segments in an endless duct and is shown in Table II. The area, length and volume have been defined. The circuit losses corresponding to each segment has been defined on the basis of an equivalent  $i^{\text{th}}$  cylindrical segment of length  $L_i$  and diameter  $D_i$  as follows

$$k_i = \text{local loss factor} = \frac{\Delta P_i}{q_i} = \frac{L_i}{D_i} \lambda_i$$

$$\lambda_i = 0.06481 - 0.01346 (\log_{10} R_i) + 0.00076 (\log_{10} R_i)$$

$$R_i = \text{Reynolds number/diameter} = \frac{\rho_i u_i D_i}{\mu}$$

This model is based on the fact that the wall surface creates a loss in the static pressure bases on wall friction coefficient. This wall friction coefficient is a function of local velocity, static pressure and temperature, viscosity and the flow Reynolds number  $R_i$  based on local diameter as the chord. The expression is based on material from reference 6. While the above model accounts for wall friction induced losses, the elements like screen, heat exchanger and the corners have extra local loss factors which need to be added. The following have been used in 0.3-m TCT modeling.

Heat exchanger	$\frac{\Delta P}{q}$ local = 4.6
Screens	$\frac{\Delta P}{q}$ local = 2
Corners	$\frac{\Delta P}{q}$ local = 0.2

The tunnel loss factor naturally varies with the amount of skin friction on exposed surfaces. For each segment of the tunnel, the local Reynolds number/local diameter is estimated and the surface skin friction losses are determined. This requires the knowledge of local static pressure, temperature and one dimensional Mach number. If the segment has extra losses, like in a corner or for a heat exchanger, the local  $\frac{\Delta P}{q}$  is added to the loss factor. Boundary layer growth features can be introduced in this model. The model articulation in the test section is treated as a tunnel circuit loss factor, where the local loss factor is a function of the model drag.

$$k_\alpha \simeq \frac{\text{wing area}}{A_{\text{test section}}} \frac{(C_{L_\alpha} \alpha)^2}{\pi A_r} \text{ where } A_r \text{ is the model aspect ratio}$$

The blockage factor varies as a function of the angle attack, the model size and its aerodynamic properties specifically the slope of lift curve. For a nonlifting body, the drag coefficient needs to be used. The sum of all the tunnel circuit loss elements result in an estimate of the pressure loss in the circuit for a given mass flow and hence the pressure ratio required at the fan for equilibrium flow. The simulation is based on the

The inlet flow in to the fan is guided through the inlet guide vane angle  $\beta_1$  resulting in fan blade inlet angle  $\beta_2$  due to fan blade movement. After the momentum is increased in the fan due to its blade properties, the fan is guided through the fan outlet guide vanes at angle  $\beta_4$ . Certain losses occur in various stages due to flow and corrections for three dimensional effects are required. After these corrections are made, the fan temperature ratio, its pressure ratio and the fan efficiency can be estimated. The numerical estimations involve calculation of the one dimensional Mach number at the inlet and outlet of blade and fixed guide vane. The Mach number estimation calls for solution to sixth order polynomial for air/nitrogen and 20th order polynomial for heavy gas sulfur hexafluoride gas. Estimations also require estimation of losses, vector component of axial flow, isentropic relation at each stage. The fan exhibits classical features of the pressure ratio having a unimodal peak corresponding to surge line. The pressure ratio vs flow characteristic with negative gradient is stable where as the positive gradient refers to instability in post surge zone.

When the gas used is the diatomic perfect gas with  $\gamma=1.4$ , the fan speed range for the tunnel can be varied depending upon the temperature of the gas. At ambient temperature, the fan speed range is 600-5000 rpm, while at 90K, the fan speed range is 600-3000 rpm. However as when the gas used is sulfur hexafluoride with a  $\gamma \simeq 1.1$ , the fan speed range is limited to 400-2400 rpm. The fan annulus diameters are 0.716 and 0.432 m. Higher speed results in the fan tip speed reaching supersonic Mach numbers.

The test section has been modeled as a 5 segment unit with top and bottom wall divergence or convergence features. The convergence allows control of Mach gradient in the test section for a given loss pattern. In a closed circuit tunnel, under steady state conditions, the pressure drop around the circuit is equal to the pressure rise in the fan. The temperature ratio across the fan is equal to the cooling contribution from heat exchanger. The net mass in the circuit remains the same. The simulation module is required to carry out the mass flow optimization so that the pressure ratio in the tunnel is zero around the full circuit. The optimization ensures that gas mass in tunnel duct remains constant unless removed out of the circuit. It also adjusts the temperature ratio in the heat exchanger to match the fan temperature rise. This is feasible while the tunnel flow remains unchoked around the circuit. As the maximum Mach number in the tunnel (usually at the test section or at tunnel choke point) the Mach number is highly sensitive to small increases in mass flow. Once choke is encountered, use of mass flow as the optimization variable is invalid. Because of the flexible wall features, the tunnel usually chokes in the test section. Typical simulation results of the tunnel providing spatial pressure profile, spatial Mach number profile, the fan speed-Mach number relation and Mach-fan power relation are shown in figures 8 through 12. The spatial profiles show the centerline total pressure and static pressure distribution as well as the one dimensional Mach number distribution, for three different gases. The power accounts for fan efficiency and is estimated on basis of temperature rise across the fan using identity  $\dot{m}_t C_p \Delta T$ .

The fan speed-Mach number profile matches with the experimental data from the tunnel for both air/Nitrogen as well as for sulfur hexafluoride. The simulation has been performed for many temperatures and the fan power estimates match the experimental results reasonably well.

However, when the  $\gamma=1.1$ , the polynomial is a 20th order equation and solution for Mach number has 9 pairs of complex and two real roots. For this tunnel, the subsonic solution is the proper solution to be used for the simulation.

The fan model used in this first version of simulation is based on a 12 blade single stage fan with fifteen fixed inlet guide vanes and ten fixed outlet guide vanes. The angle  $\beta_1$  in the inlet velocity triangle below corresponds to fixed inlet vanes. The angle  $\beta_4$  in the exit velocity triangle corresponds to fixed outlet vanes.

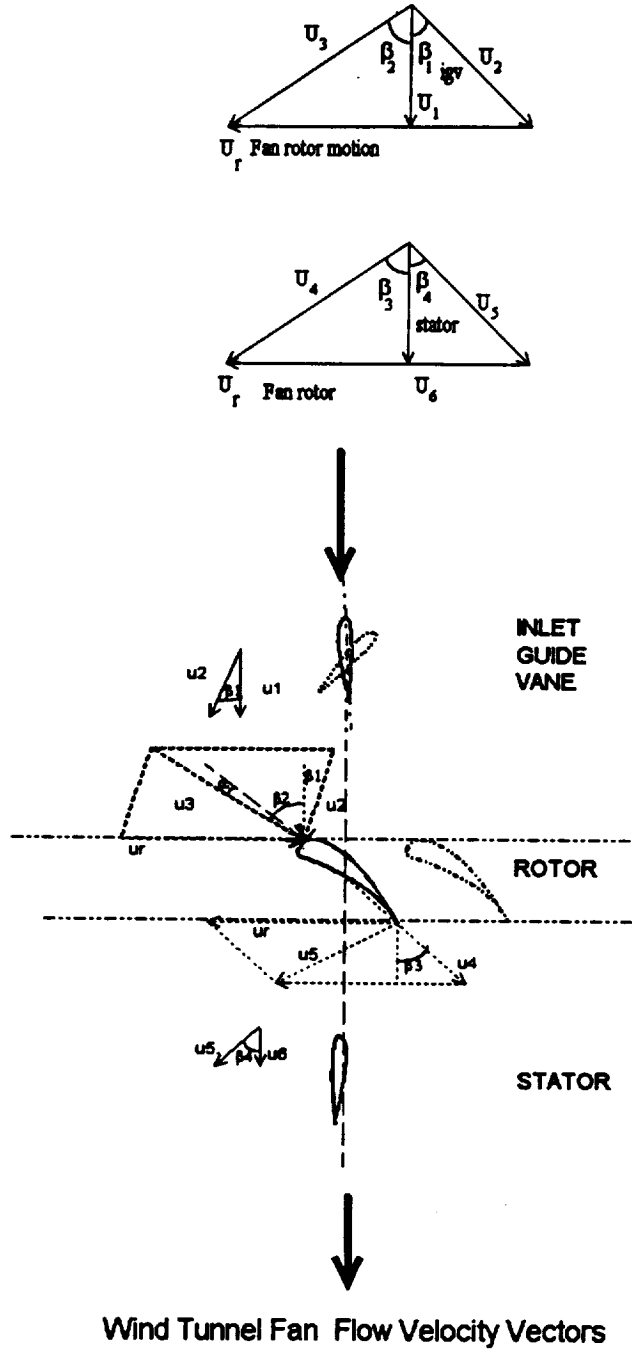


**Table II: 0.3-m TCT Geometrical data**

Dist m	Area m <sup>2</sup>	Volume m <sup>3</sup>	
0.000	0.254	0.254	Fan exit
0.635	0.282	0.179	
1.245	0.357	0.217	
1.854	0.437	0.266	
2.641	0.516	0.406	
3.251	0.566	0.345	
4.471	0.816	0.995	
5.690	1.006	1.226	Heat exchanger
6.299	1.108	0.675	
6.908	1.168	0.711	
8.483	1.168	1.840	
9.956	1.162	1.716	Second Corner
11.33	1.149	1.581	
11.43	1.112	0.111	
11.53	1.042	0.104	Third corner
11.63	0.948	0.0948	
11.73	0.833	0.0833	
11.83	0.719	0.0719	
11.93	0.597	0.0597	
12.03	0.496	0.0496	
12.14	0.404	0.0404	
12.24	0.328	0.0328	
12.34	0.267	0.0267	
12.44	0.219	0.0219	
12.54	0.178	0.0184	
12.64	0.148	0.0173	
12.75	0.123	0.0138	
12.85	0.113	0.0129	
12.95	0.109	0.0125	Flexible wall test section
13.05	0.109	0.0209	
13.22	0.109	0.0370	
13.52	0.109	0.0370	
13.82	0.109	0.0395	
14.14	0.115	0.0137	
14.25	0.130	0.0350	
14.52	0.145	0.0188	
14.65	0.152	0.0820	
15.19	0.189	0.0850	
15.64	0.210	0.0440	
15.85	0.240	0.1104	High speed Diffuser
16.31	0.284	0.1278	
16.76	0.330	0.1518	
17.22	0.379	0.1743	Fourth corner
17.67	0.434	0.1996	
18.13	0.455	0.5500	
19.35	0.455	0.5550	First corner
20.57	0.394	0.2837	
21.29	0.253	0.2530	Fan entry

## References

1. Goodyer, M. J. and Kilgore, R. A.; High Reynolds Number Cryogenic Wind Tunnel, AIAA Journal, Volume 11, No. 5, May 1973, pp 613-619.
2. Gloss, B. B.; Initial Research Program for the National Transonic Facility, AIAA Paper 84-0585, AIAA 13th Aerodynamic Testing Conference San Diego, California 1984.
3. Balakrishna, S. and Kilgore, W.A., : Modeling and Control Study of the NASA 0.3-Meter Transonic Cryogenic Tunnel for Use with Sulfur Hexafluoride Medium. NASA CR 189737 : December 1992.
4. Balakrishna, S.; Synthesis of a Control Model for a Liquid Nitrogen Cooled, Closed Circuit, Cryogenic Nitrogen Wind Tunnel and its Validation, NASA CR 162508, February 1980.
5. Balakrishna, S. and Kilgore, W. A.; Microcomputer base Controller for the Langley 0.3-Meter Transonic Cryogenic Tunnel, NASA CR 181808, March 1989.
6. Pope, A.; Wind Tunnel Testing, John Wiley Publications, 1954.
7. Critical Design Review Document, NASA LaRC 1/3 M-Transonic Cryogenic Tunnel Modification Study to Use Heavy Gas Test Media, Sverdrup Technology, Inc, April 1992.

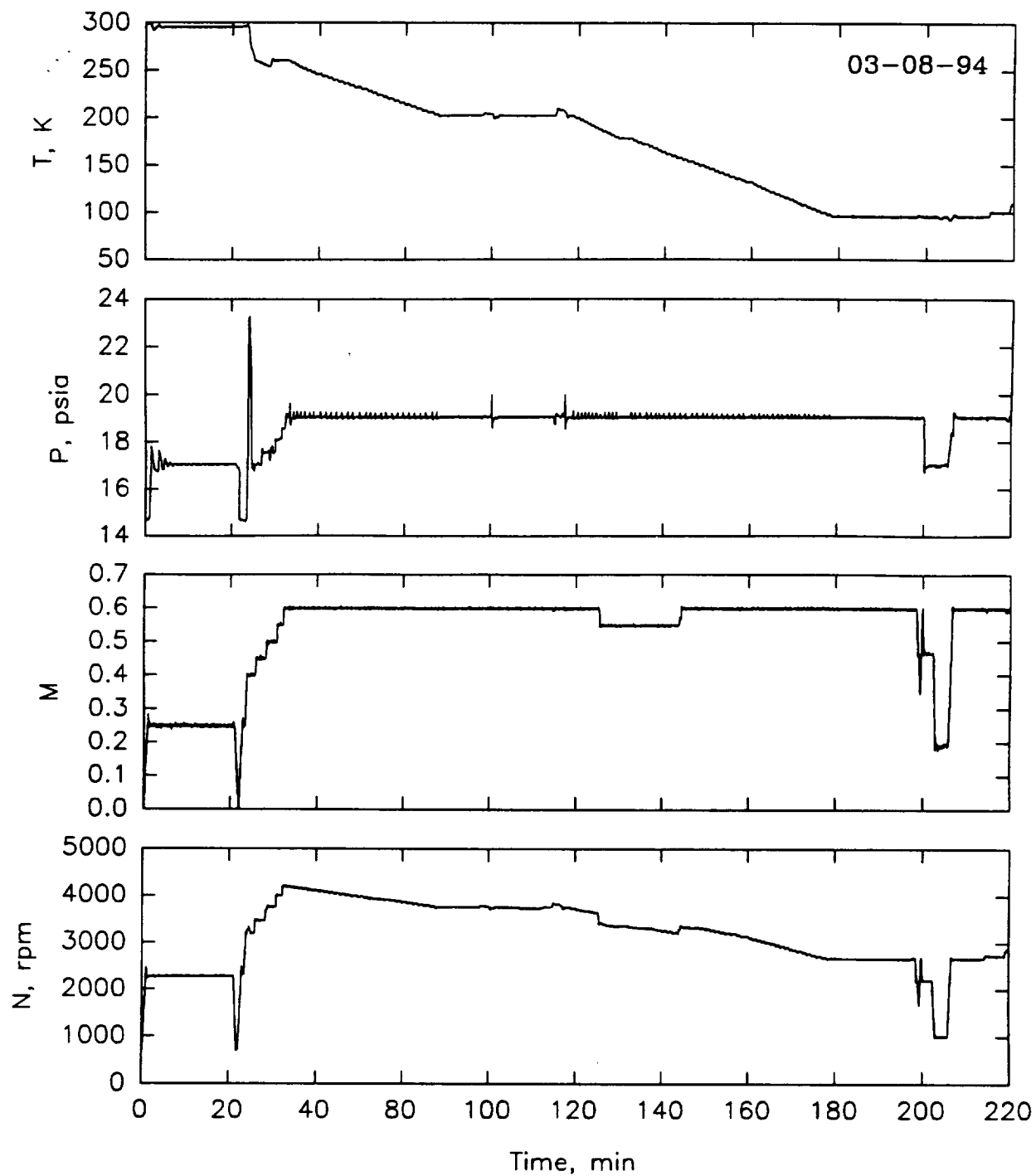


Figure 2. Cryo Mode Operation of 0.3-m TCT with Heat Exchanger

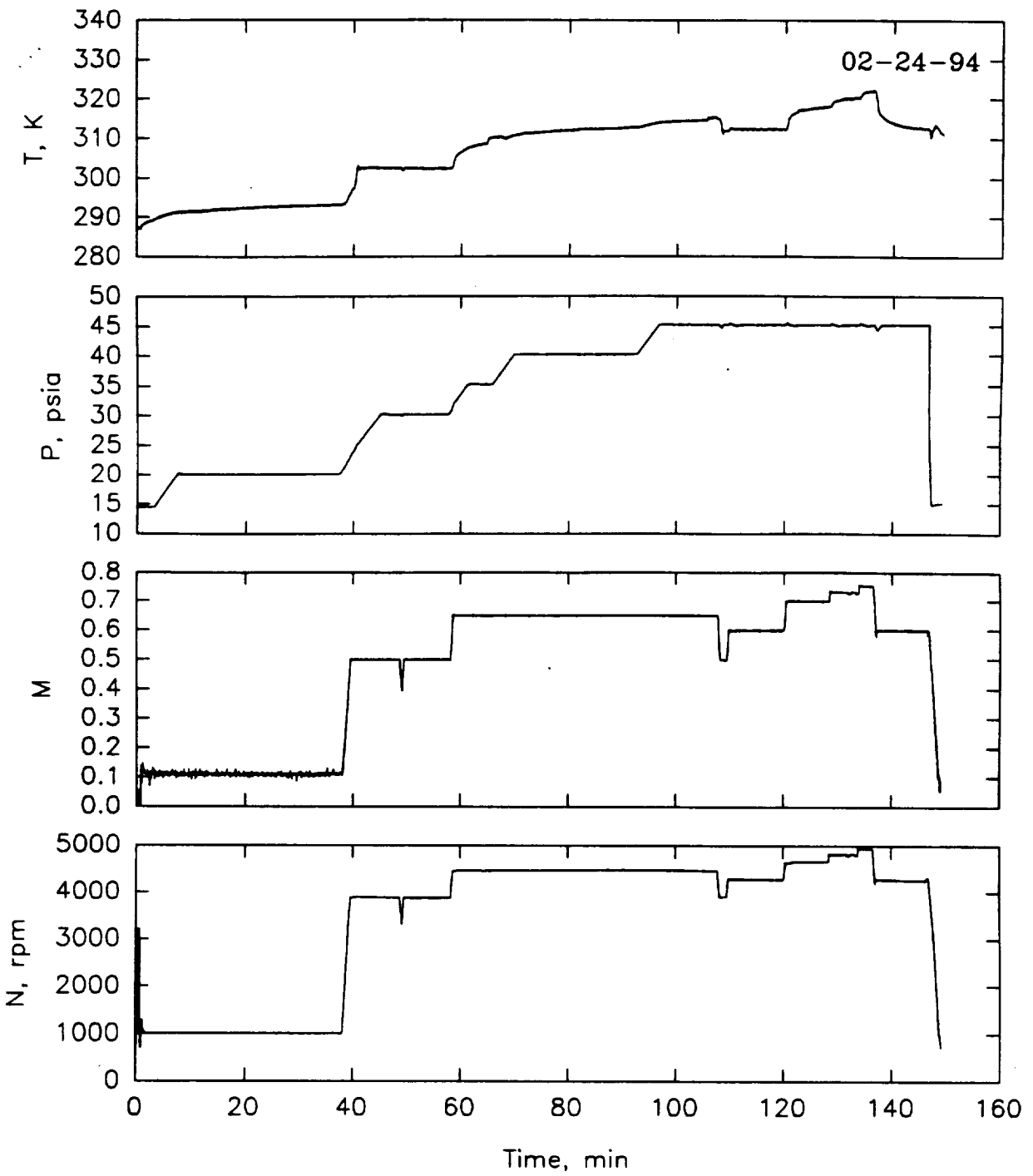


Figure 1. Air Mode Operation of 0.3-m TCT with Heat Exchanger

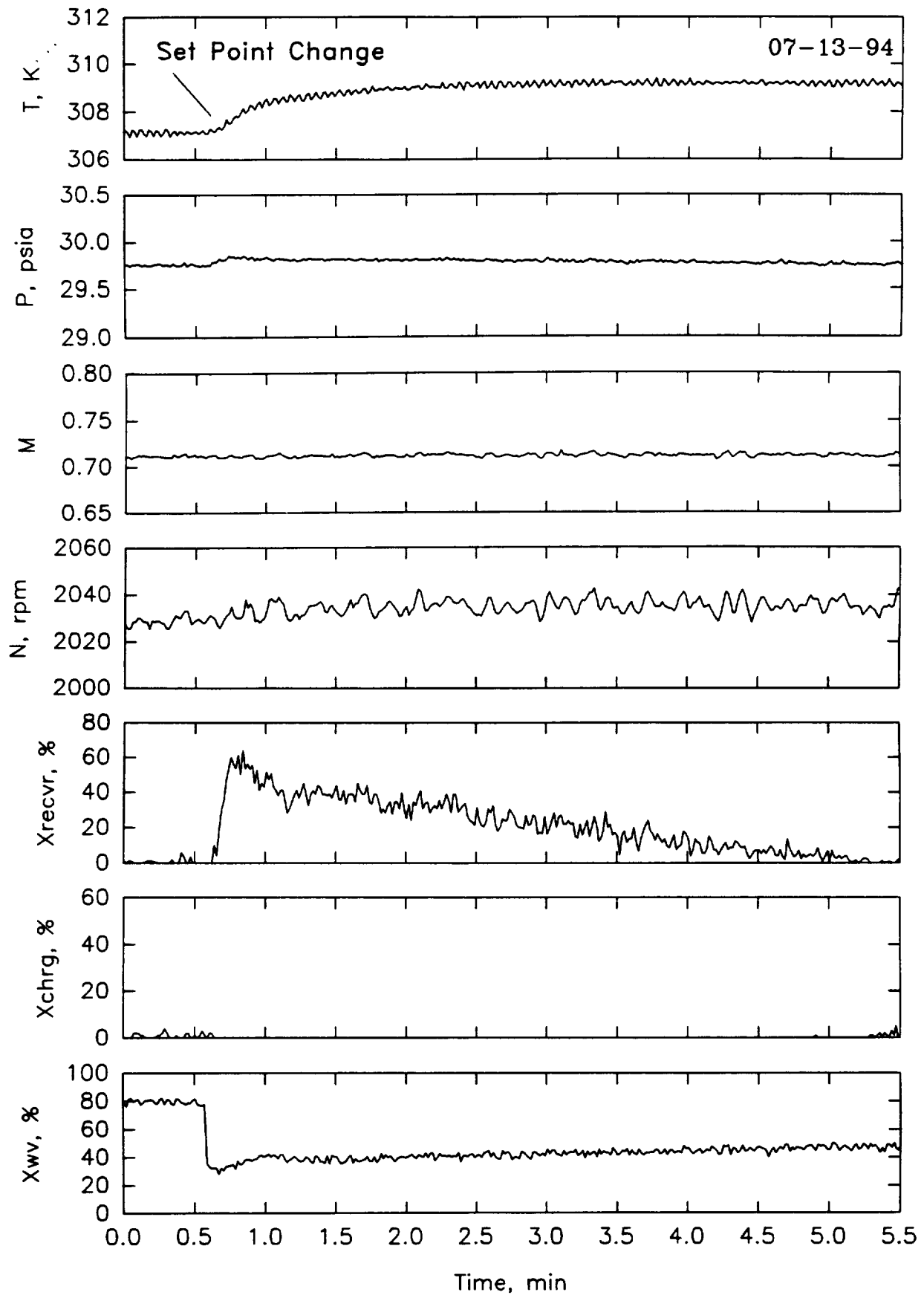


Figure 4. Temperature Set Point Change (SF6 Mode)

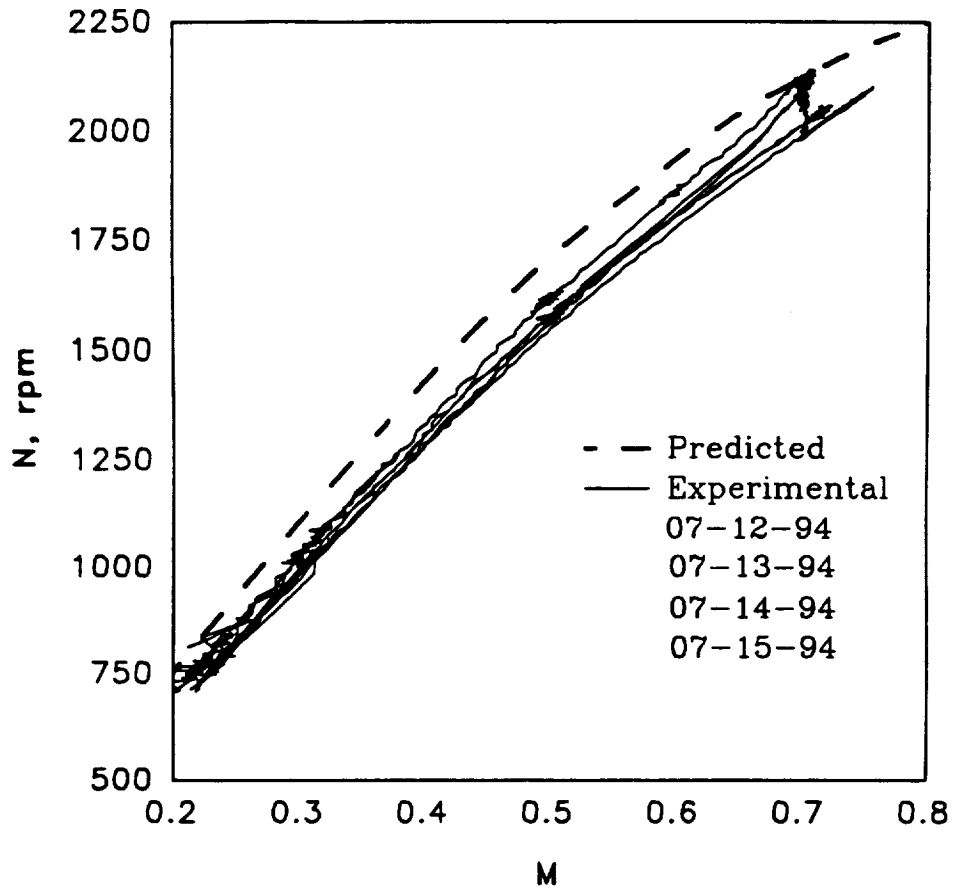


Figure 3. Fan Map of 0.3-m TCT with SF6

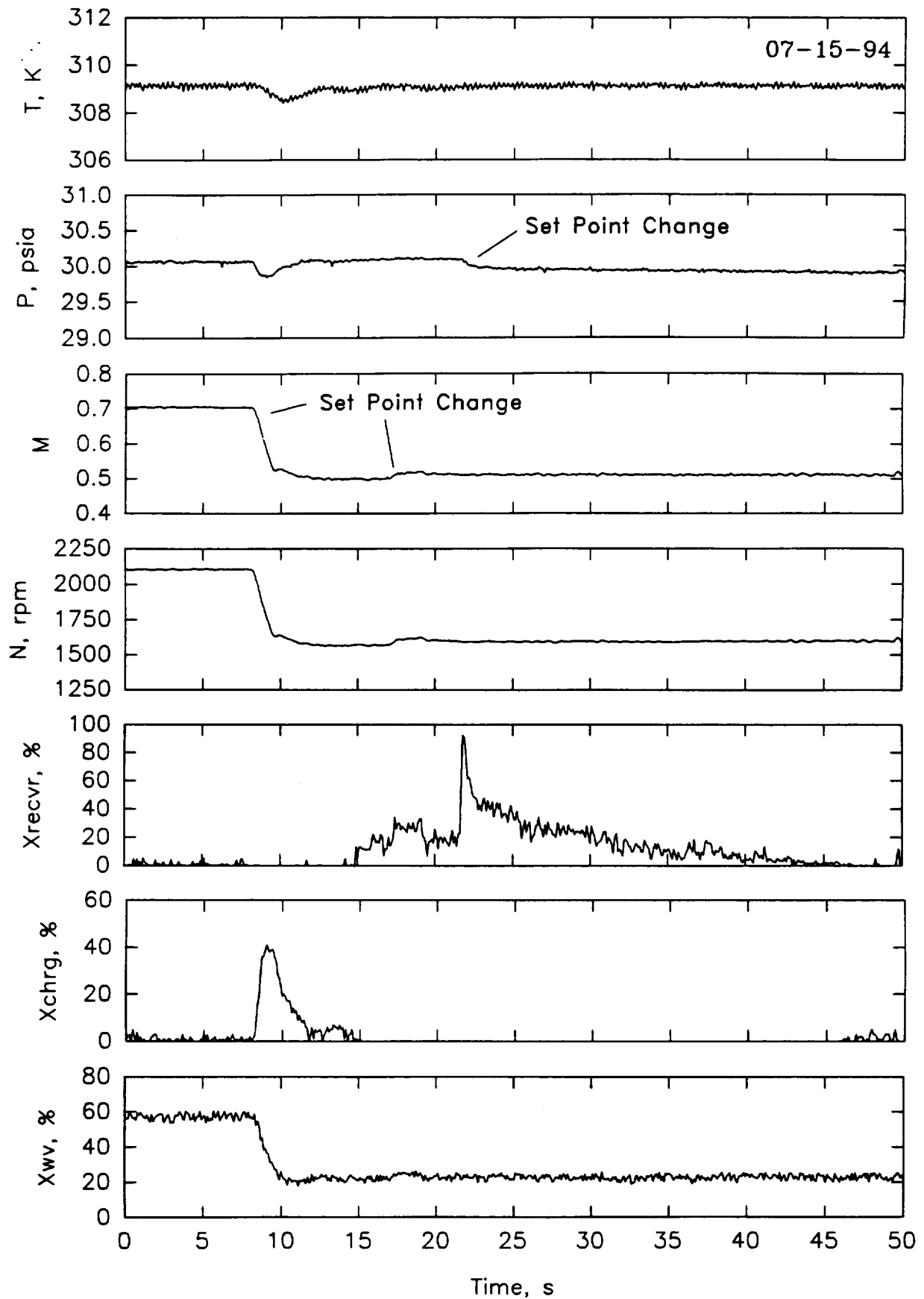


Figure 5. Pressure and Mach No. Set Point Change (SF6 Mode)

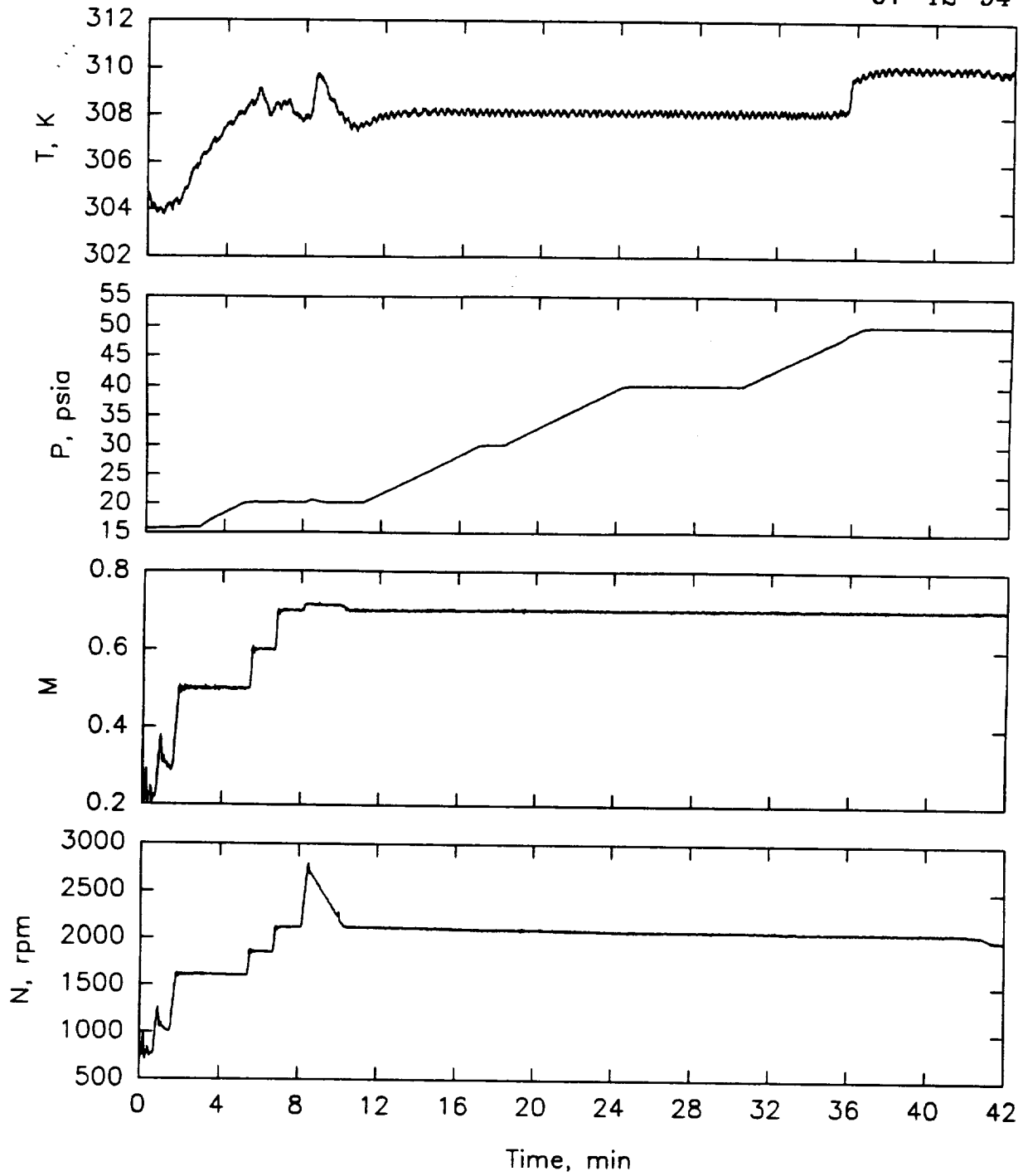


Figure 6. Pressure and Mach No. Set Point Change (SF6 Mode)

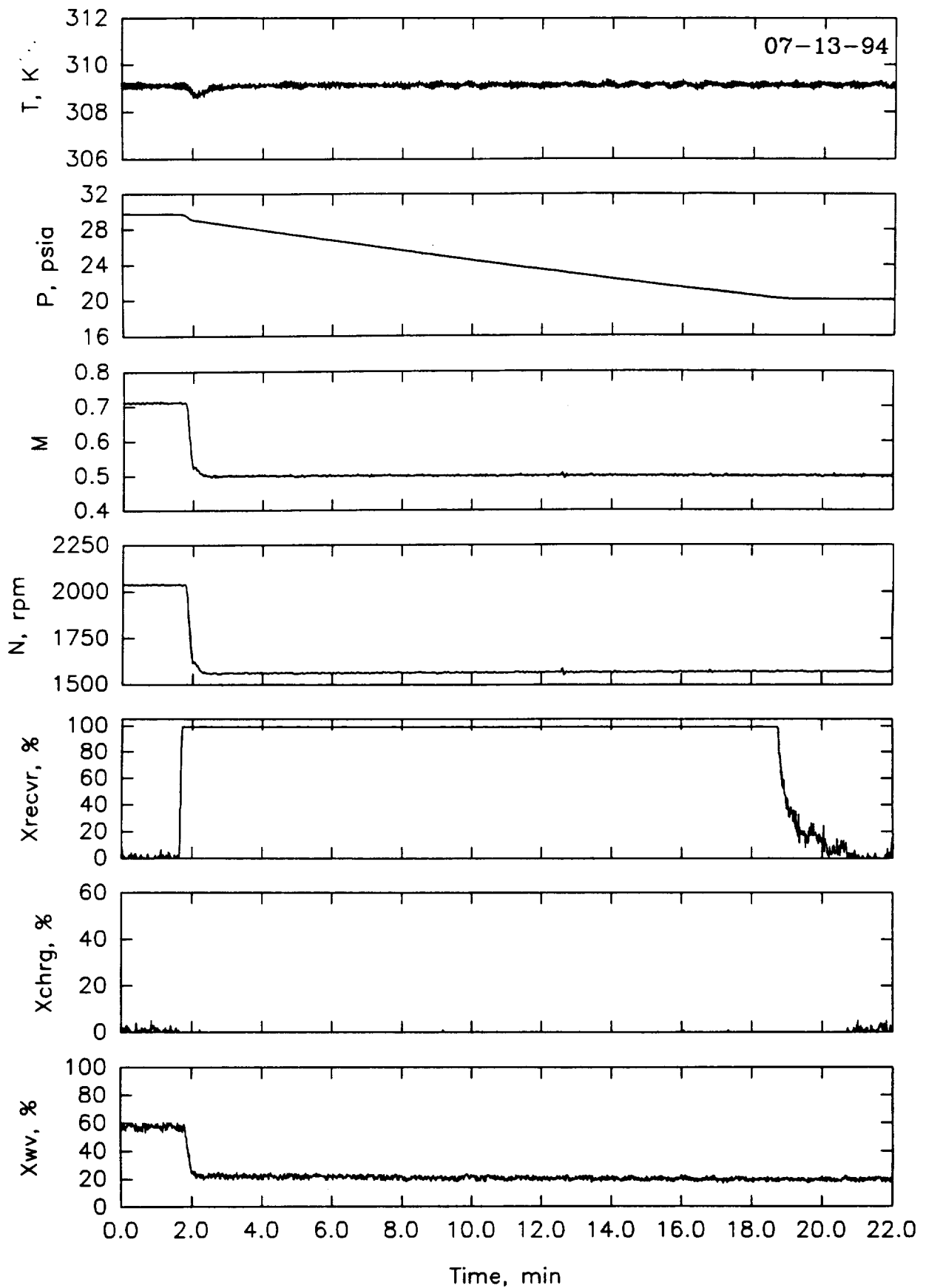


Figure 7. Pressure and Mach No. Set Point Change (SF6 Mode)

Figure 8: Air mode operation of 0.3-m TCT- Simulation & Experiments

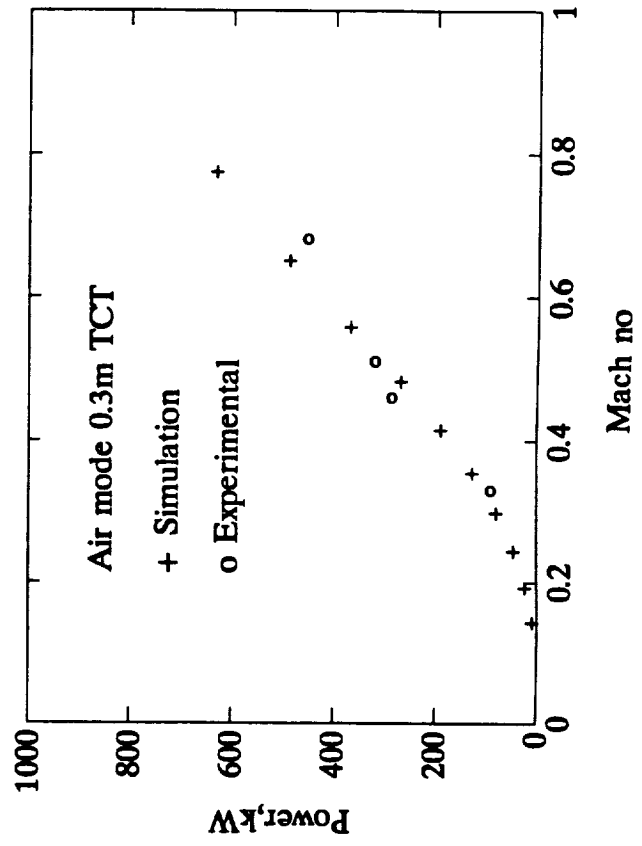
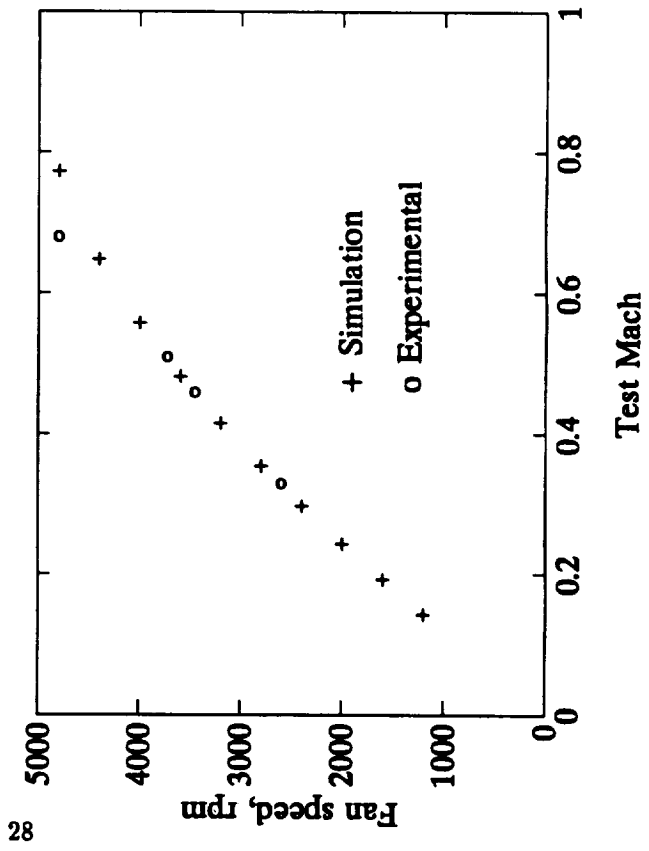
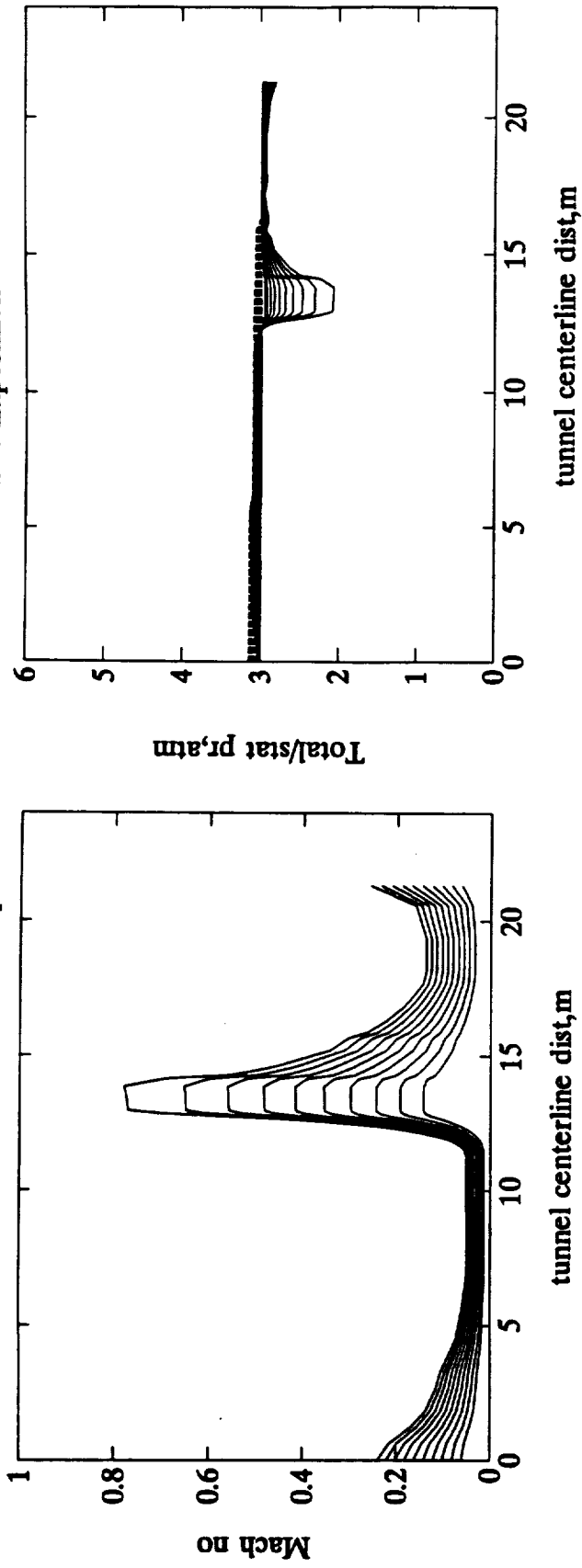


Figure 9: Air mode operation of 0.3-m TCT- Simulation & Experiments

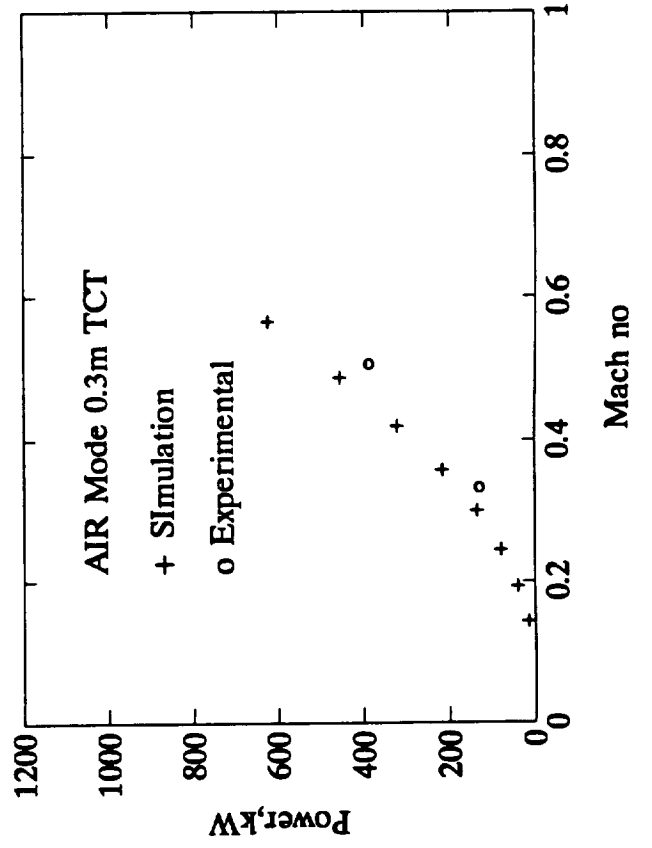
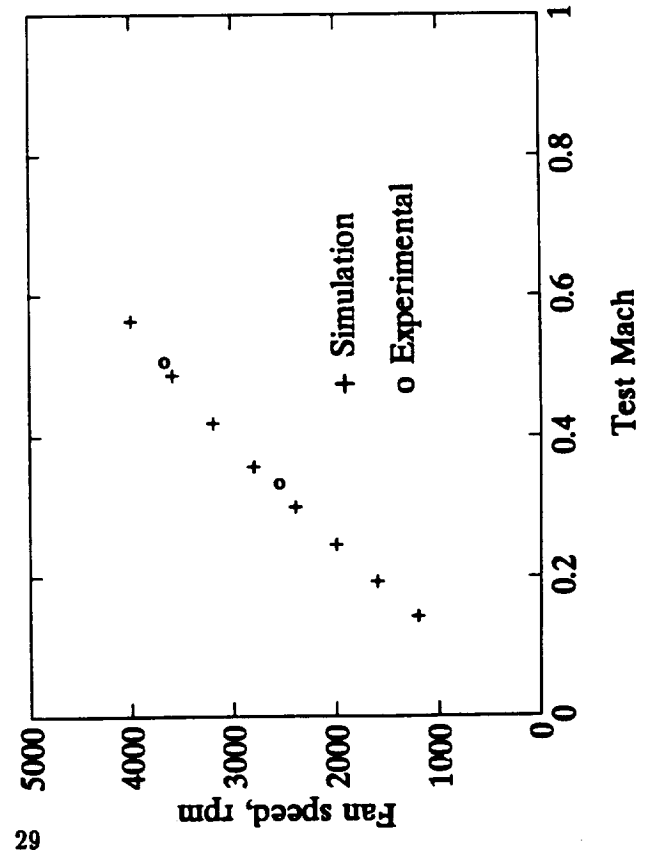
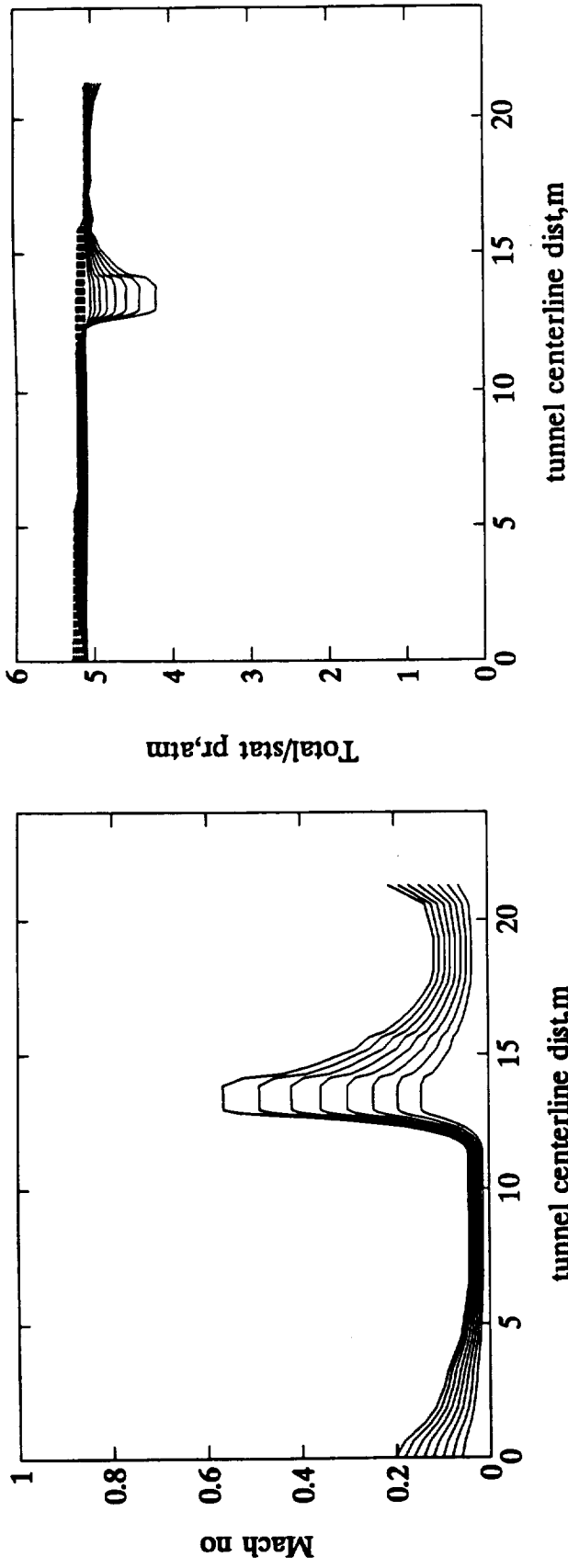
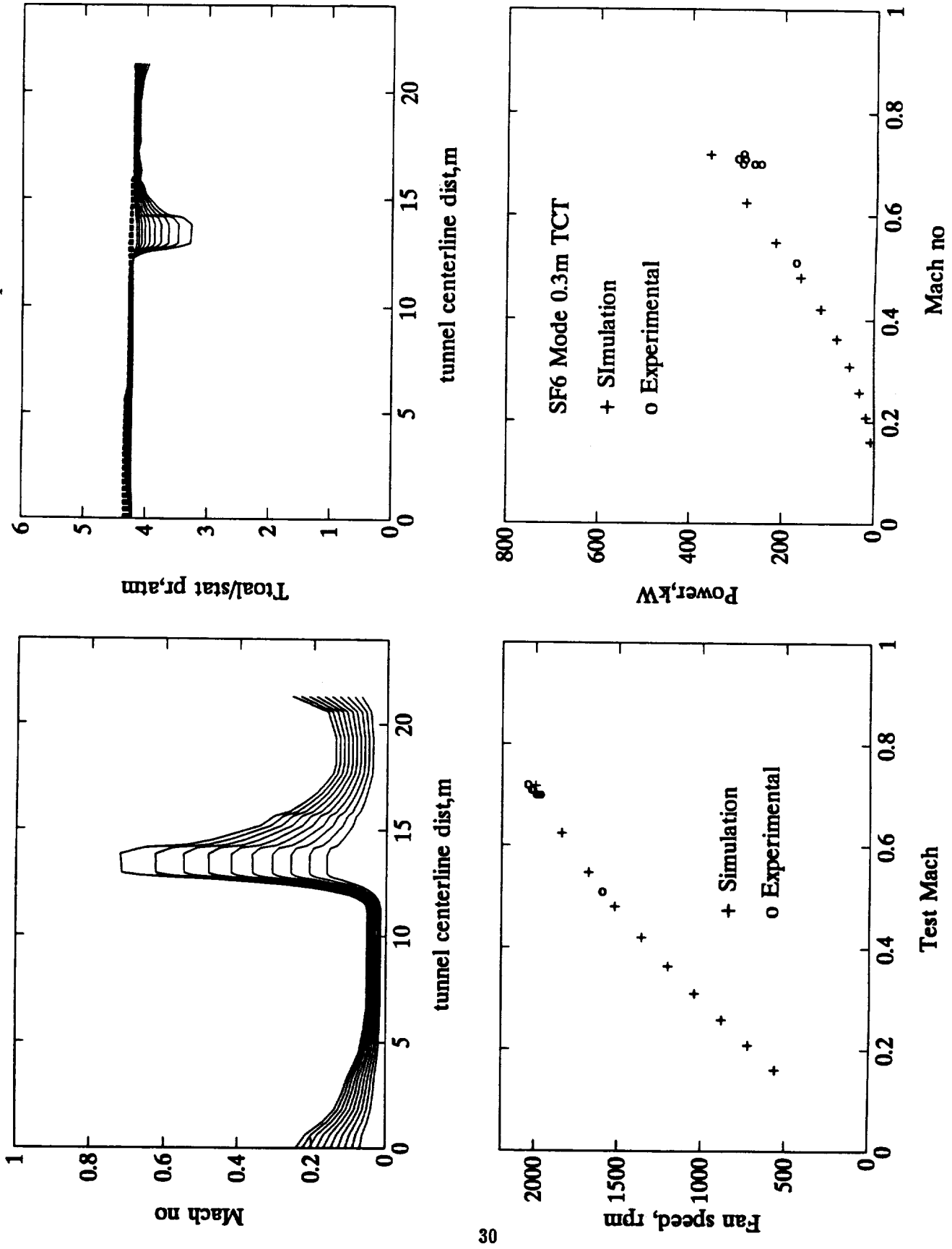


Figure 10: SF6 mode operation of 0.3-m TCT- Simulation & Experiment



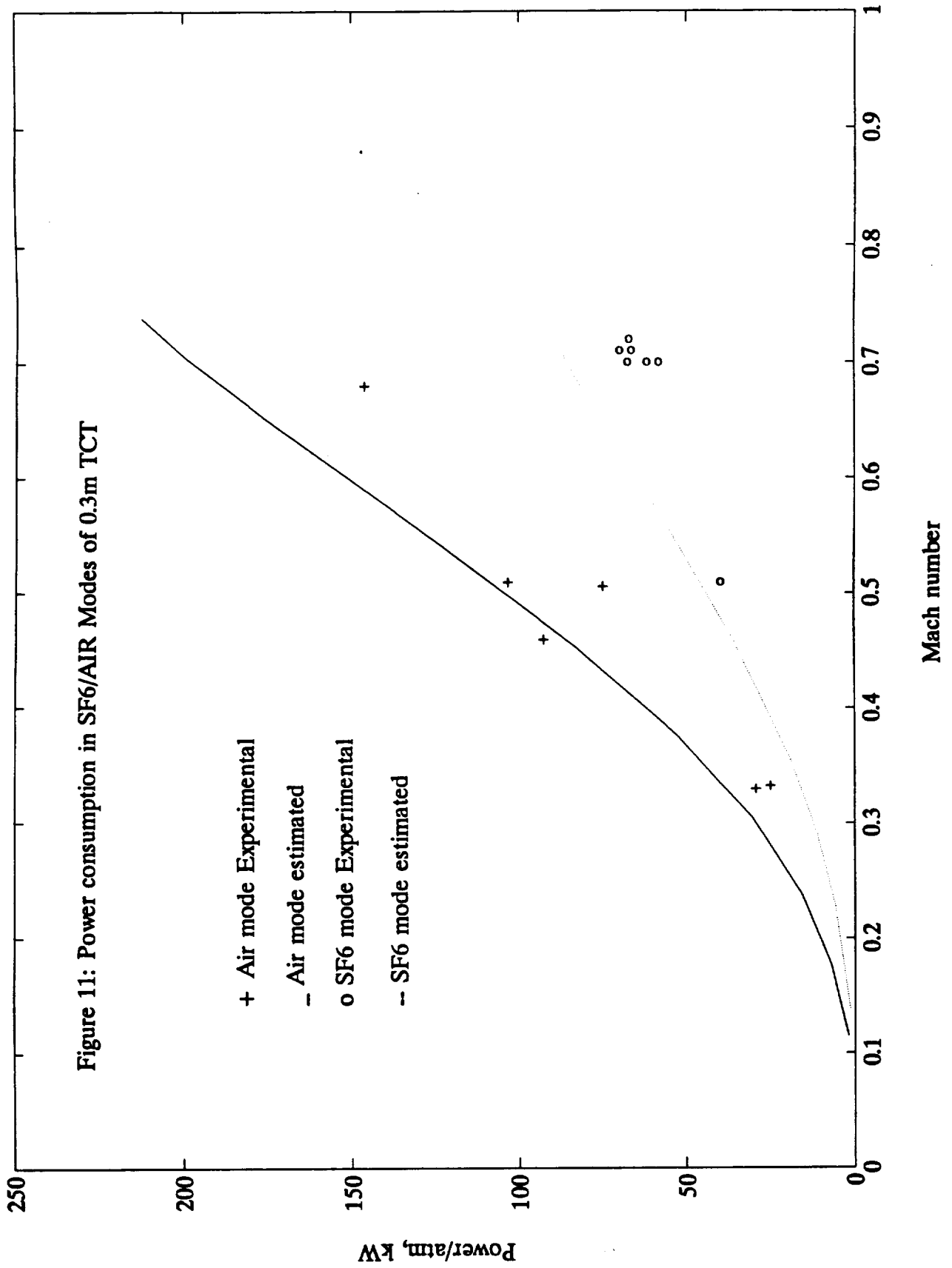
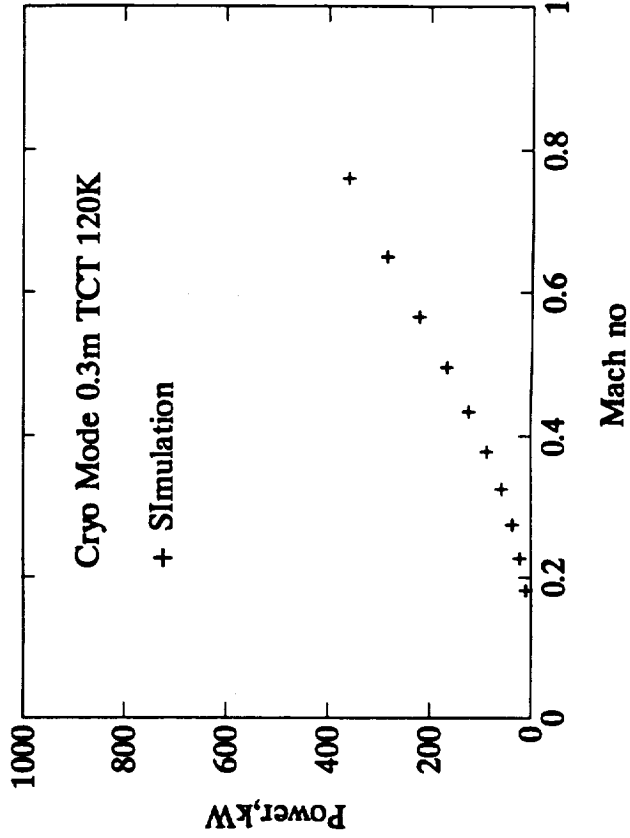
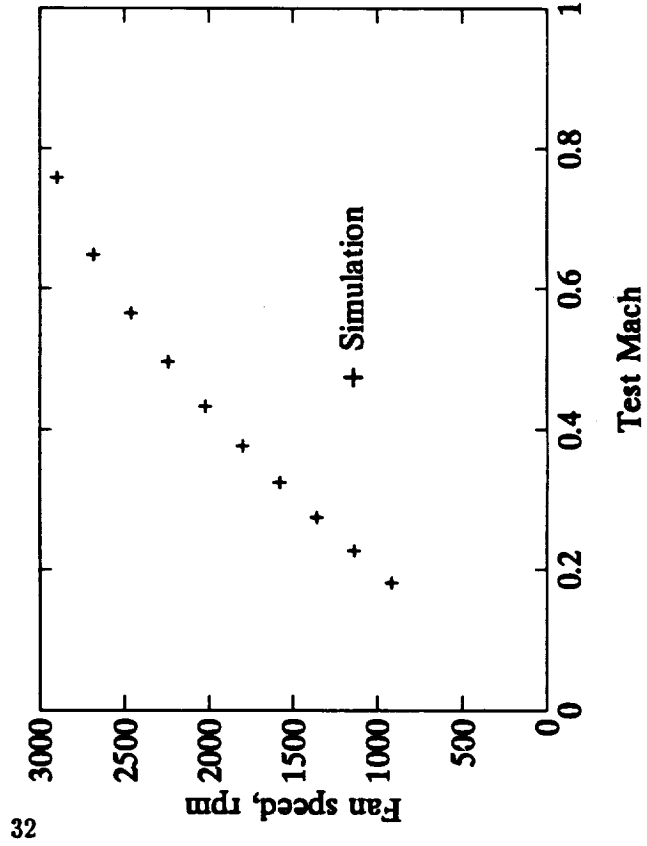
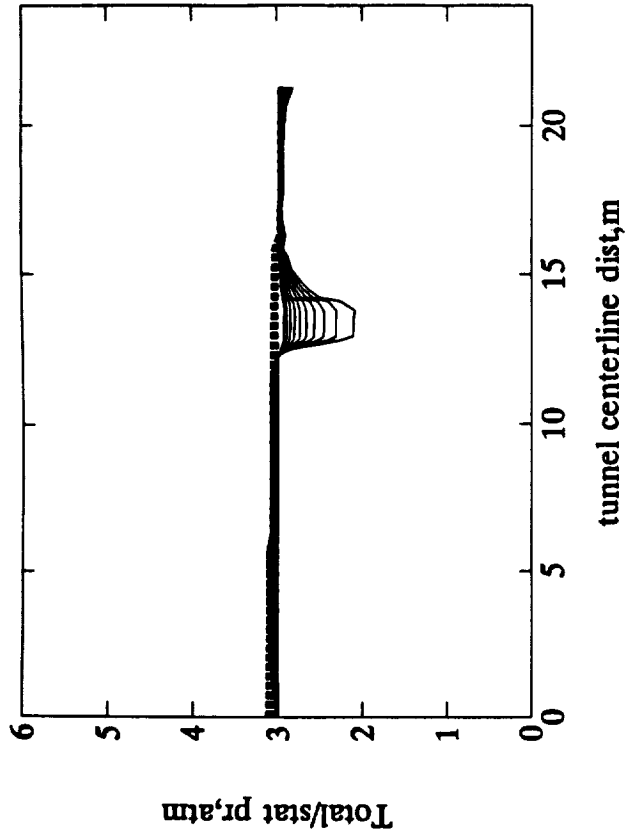
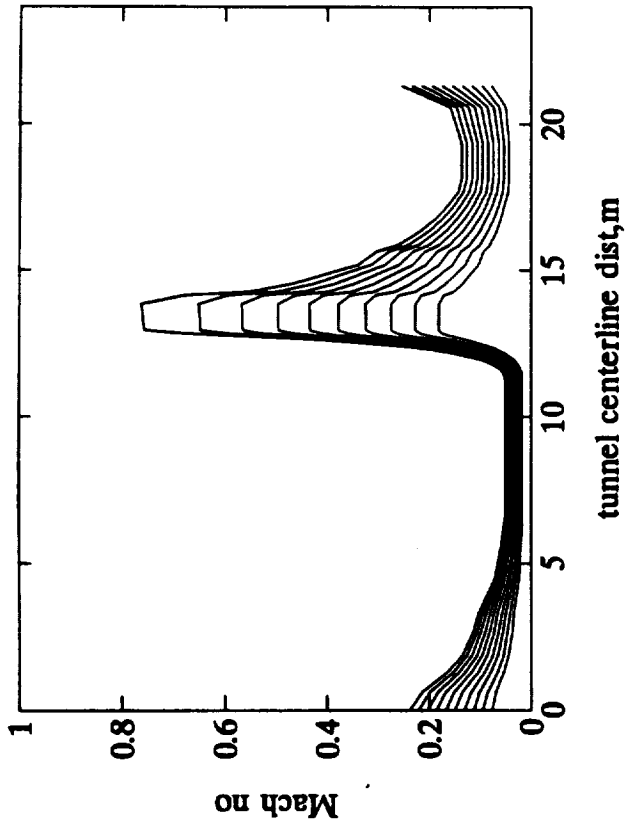


Figure 12: SF6 mode operation of 0.3-m TCT- Simulation



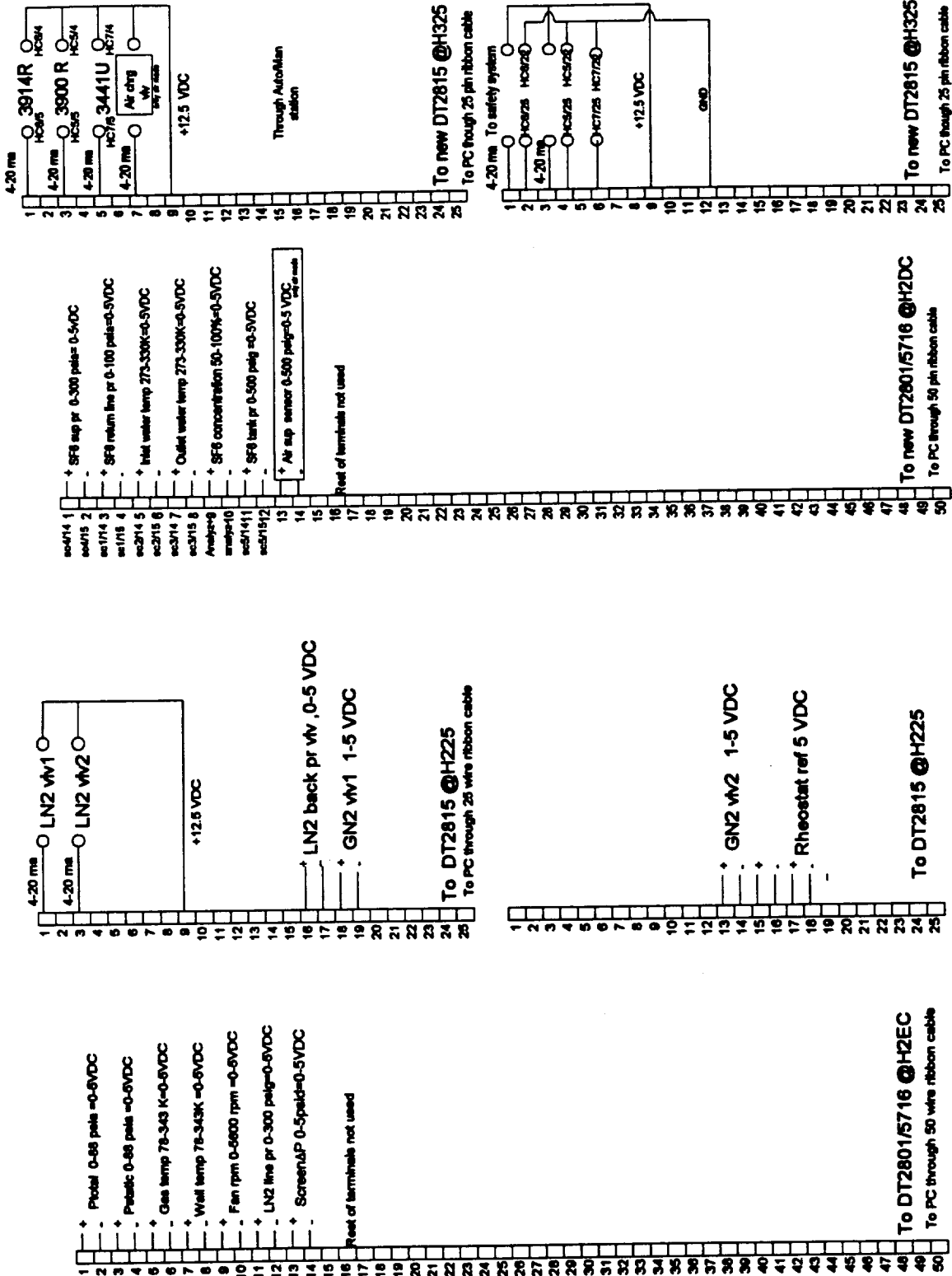


Figure 13: The 0.3 m TCT Cryo/Air/SF6 controller wiring - 1994

# REPORT DOCUMENTATION PAGE

Form Approved  
OMB No. 0704-0188

Public reporting burden for this collection of information is estimated to average 1 hour per response, including the time for reviewing instructions, searching existing data sources, gathering and maintaining the data needed, and completing and reviewing the collection of information. Send comments regarding this burden estimate or any other aspect of this collection of information, including suggestions for reducing this burden, to Washington Headquarters Services, Directorate for Information Operations and Reports, 1215 Jefferson Davis Highway, Suite 1204, Arlington, VA 22202-4302, and to the Office of Management and Budget, Paperwork Reduction Project (0704-0188), Washington, DC 20503.

1. AGENCY USE ONLY (Leave blank)		2. REPORT DATE <p style="text-align: center;">January 1995</p>		3. REPORT TYPE AND DATES COVERED <p style="text-align: center;">Contractor Report</p>	
4. TITLE AND SUBTITLE <p>Performance of the 0.3-Meter Transonic Cryogenic Tunnel With Air, Nitrogen, and Sulfur Hexafluoride Media Under Closed Loop Automatic Control</p>				5. FUNDING NUMBERS <p>C NAS1-19672 WU 505-59-50-02</p>	
6. AUTHOR(S) <p>S. Balakrishna W. Allen Kilgore</p>				8. PERFORMING ORGANIZATION REPORT NUMBER	
7. PERFORMING ORGANIZATION NAME(S) AND ADDRESS(ES) <p>ViGYAN, Inc. 30 Research Drive Hampton, VA 23666-1225</p>					
9. SPONSORING / MONITORING AGENCY NAME(S) AND ADDRESS(ES) <p>National Aeronautics and Space Administration Langley Research Center Hampton, VA 23681-0001</p>				10. SPONSORING / MONITORING AGENCY REPORT NUMBER <p style="text-align: center;">NASA CR-195052</p>	
11. SUPPLEMENTARY NOTES <p>Langley Technical Monitor: J. B. Anders</p>					
12a. DISTRIBUTION / AVAILABILITY STATEMENT <p>Unclassified - Unlimited  Subject Category - 34</p>				12b. DISTRIBUTION CODE	
13. ABSTRACT (Maximum 200 words) <p>The NASA Langley 0.3-m Transonic Cryogenic Tunnel has been modified in 1994, to operate with any one of the three test gas media viz., air, cryogenic nitrogen gas, or sulfur hexafluoride gas. This document provides the initial test results with respect to the tunnel performance and tunnel control, as a part of the commissioning activities on the microcomputer based controller. The tunnel can provide precise and stable control of temperature to <math>\leq \pm 0.3K</math> in the range 80-320 K in cyro mode or 300-320 K in air/SF6 mode, pressure to <math>\pm 0.01</math> psia in the range 15-88 psia and Mach number to <math>\pm 0.0015</math> in the range 0.150 to transonic Mach numbers up to 1.000. A new heat exchanger has been included in the tunnel circuit and is performing adequately. The tunnel airfoil testing benefits considerably by precise control of tunnel states and helps in generating high quality aerodynamic test data from the 0.3-m TCT.</p>					
14. SUBJECT TERMS <p>High Reynolds Number                      Heavy Gas Wind Tunnel Tunnel closed Loop Control              Tunnel Performance</p>				15. NUMBER OF PAGES <p style="text-align: center;">34</p>	
17. SECURITY CLASSIFICATION OF REPORT <p style="text-align: center;">Unclassified</p>				16. PRICE CODE <p style="text-align: center;">A03</p>	
				20. LIMITATION OF ABSTRACT	
18. SECURITY CLASSIFICATION OF THIS PAGE <p style="text-align: center;">Unclassified</p>		19. SECURITY CLASSIFICATION OF ABSTRACT <p style="text-align: center;">Unclassified</p>			